3-2016

Nitrogen sources and net growth efficiency of zooplankton in three Amazon River plume food webs

Natalie Loick-Wilde

Sarah C. Weber

Brandon J. Condon
Virginia Institute of Marine Science

Douglas G. Capone

Victoria J. Coles

See next page for additional authors

Recommended Citation

Loick-Wilde, Natalie; Weber, Sarah C.; Condon, Brandon J.; Capone, Douglas G.; Coles, Victoria J.; Medeiros, Patricia M.; Steinberg, Deborah K.; and Montoya, Joseph P., Nitrogen sources and net growth efficiency of zooplankton in three Amazon River plume food webs (2016). *Limnology and Oceanography*, 61(2), 460-481.
doi: 10.1002/lno.10227

LIMNOLOGY
and
OCEANOGRAPHY

ASLO

Limnol. Oceanogr. 61, 2016, 460–481

doi: 10.1002/lno.10227

Nitrogen sources and net growth efficiency of zooplankton in three Amazon River plume food webs

Natalie Loick-Wilde,[a,*1] Sarah C. Weber,[1] Brandon J. Conroy,[2] Douglas G. Capone,[3] Victoria J. Coles,[4] Patricia M. Medeiros,[5] Deborah K. Steinberg,[2] Joseph P. Montoya[1]

[1]School of Biology at Georgia Institute of Technology, Atlanta, Georgia
[2]Virginia Institute of Marine Science, College of William & Mary, Gloucester Point, Virginia
[3]University of Southern California, Los Angeles, California
[4]University of Maryland Center for Environmental Science, Horn Point Laboratory, Cambridge, Maryland
[5]Department of Marine Sciences, University of Georgia, Athens, Georgia

Abstract

The plasticity of nitrogen specific net growth efficiency (NGE) in marine mesozooplankton is currently unresolved, with discordant lines of evidence suggesting that NGE is constant, or that it varies with nitrogen source, food availability, and food quality in marine ecosystems. Specifically, the fate of nitrogen from nitrogen fixation is poorly known. We use ^{15}N : ^{14}N ratios in plankton in combination with hydrological data, nutrient profiles, and nitrogen fixation rate measurements to investigate the relationship between new nitrogen sources and the nitrogen specific NGE in three plankton communities along the outer Amazon River plume. The NGE of small (200–500 μm) mesozooplankton was estimated from the $\delta^{15}N$ differences between particulate nitrogen and zooplankton using an open system Rayleigh fractionation model. The transfer efficiency of nitrogen among larger (> 500 μm) mesozooplankton was estimated from the change in $\delta^{15}N$ as a function of zooplankton size. The Amazon River was not a significant source of bioavailable nitrogen anywhere in our study region, and subsurface nitrate was the primary new nitrogen source for the outer shelf community, which was dominated by diatoms. N_2 fixation was the principal new nitrogen source at sites of high diatom diazotroph association abundance and at oceanic sites dominated by *Trichodesmium* spp. and *Synechococcus* spp. Although we found clear spatial differences in food quantity, food quality, and diazotroph inputs into mesozooplankton, our data show no significant differences in mesozooplankton nitrogen transfer efficiency and NGE (for latter, mean ± SD: 59 ± 10%) among sites.

The movement of new nitrogen through pelagic food webs is critical to marine secondary production and the efficiency of nitrogen transfer may be especially sensitive to changes in phytoplankton community structure associated with climate change (Hutchins et al. 2007; Paerl and Huisman 2008). In zooplankton, the proportion of assimilated nitrogen that is used for growth is called the nitrogen net growth efficiency (NGE), a critical, but poorly constrained parameter in biogeochemical models (Touratier et al. 2001; Anderson et al. 2013; Mitra et al. 2014). A variety of controlled laboratory experiments (Checkley 1980; Berggreen et al. 1988; Kiorboe 1989) suggest that zooplankton NGE is consistently around 45% (Touratier et al. 1999; Touratier et al. 2001), while field studies suggest that NGE is much more variable, ranging from 18% to 72% (Le Borgne 1982 and references therein), and sensitive to food quality as shown by the model of Anderson and Hessen (1995).

The movement of nitrogen (N) through the phytoplankton into the mesozooplankton community can be tracked and quantified by means of stable nitrogen isotope analysis (Peterson and Fry 1987). The natural abundance of stable nitrogen isotopes in plankton reflects the sources of N supporting biological production, as well as the physiological processes that may alter isotopic abundance within the ecosystem (Montoya et al. 2002; Martínez Del Rio et al. 2009). The $\delta^{15}N$ (‰ deviation in ^{15}N : ^{14}N between a sample and atmospheric N_2) of

[a]Present address: Leibniz-Institute for Baltic Sea Research Warnemuende, Rostock, Germany
*Correspondence: natalie.loick-wilde@io-warnemuende.de

Additional Supporting Information may be found in the online version of this article.

mesozooplankton and particulate organic nitrogen (PN) in particular reflect the origin, movement, and transformation of nitrogen in the upper water column (Goering et al. 1990; Fry and Quiñones 1994; Benner et al. 1997).

The NGE of mesozooplankton can be estimated from the difference in the $\delta^{15}N$ of mesozooplankton and PN ($\Delta\delta$) if the physiological processes that fractionate the nitrogen isotopes are accounted for (Montoya 2007; Montoya 2008). The release of ^{15}N-depleted ammonium (NH_4^+) through excretion appears to play a pivotal role in enriching an animal's tissues in ^{15}N, typically by 2‰–4‰ relative to its diet (Minagawa and Wada 1984; Bada et al. 1989; Gannes et al. 1997).

The major factors that can affect NH_4^+ excretion rates of ammonotelic (ammonium excreting) zooplankton include temperature, body size, nutritional status, food quality, light, and salinity, whereas the principal feeding mode (e.g., carnivory, herbivory, or detrivory) does not appear to have a strong effect on excretion rate (reviewed by Steinberg and Saba 2008). From a physiological point of view, the increase in $\delta^{15}N$ with trophic position (trophic effect) results from the partitioning of assimilated dietary nitrogen between new biomass and NH_4^+ excretion (Montoya 2008). In other words, the greater the fraction of assimilated nitrogen released through excretion, the greater the trophic effect and the higher the resulting $\delta^{15}N$ of the animal's biomass.

PN and mesozoplankton differ in their turnover times and in the type of information they provide on ecological processes over time scales of hours to weeks (Montoya 2007). The $\delta^{15}N$ of PN is sensitive to the sources of N (e.g., nitrate, ammonium, N_2) and the uptake mechanisms supporting production (Minagawa and Wada 1986; Carpenter et al. 1997; Waser et al. 2000). This baseline $\delta^{15}N$ can be modified by transient events including phytoplankton blooms driven by the injection of subthermocline nitrate into surface waters or by inputs of regenerated ammonium from heterotrophs (Altabet 1989; Waser et al. 2000). Repeated sampling of PN in the water column and vertical integration of the $\delta^{15}N$ of PN can provide a measure of the average isotopic state of the upper water column (Altabet and McCarthy 1985; Montoya et al. 2002; Montoya 2007). The $\delta^{15}N$ of zooplankton integrates over longer time scales that reflect animal growth rates, and is, therefore, less sensitive to transient events than the $\delta^{15}N$ of PN (Montoya 2007). The difference in $\delta^{15}N$ between PN and zooplankton at any time is thus a time-averaged value that reflects the cumulative impact of the animal's feeding and excretory processes over the animal's characteristic N turnover time. This in turn provides an estimate of the "time integrated" NGE in the planktonic food web (Montoya 2007).

A number of lines of isotopic evidence indicate that the incorporation of nitrogen from diazotrophic (N_2-fixing) phytoplankton into mesozooplankton at oligotrophic sites is highly efficient, and may be more efficient than zooplankton incorporation of nitrogen from phytoplankton supported by nitrate in more eutrophic waters. For the tropical North Atlantic, relevant observations include high in situ incorporation rates of diazotroph nitrogen into mesozooplankton (O'Neil et al. 1995), small differences in $\delta^{15}N$ among zooplankton size fractions (Montoya et al. 2002), and correlations between $\delta^{15}N$ values of amino acids from *Trichodesmium* and various zooplankton size fractions (McClelland et al. 2003). Furthermore, high in situ diazotroph nitrogen incorporation rates into the amino acid nitrogen of mesozooplankton have been observed in the Baltic Sea (Loick-Wilde et al. 2012).

Diverse N_2 fixing communities occur in tropical river-ocean systems like the Amazon or Mekong River plumes, where multiple allochthonous and autochthonous nitrogen sources may be important (Voss et al. 2006; Foster et al. 2007; Moisander et al. 2008). In such dynamic systems, a variety of hydrographic (e.g., T, S, nutrient concentrations), biological (e.g., community composition and rates of activity), and biogeochemical (e.g., $\delta^{15}N$ and $\delta^{13}C$) measurements provide insight into the dominant organic and inorganic N sources supporting different plankton communities (Fry and Sherr 1984; Voss et al. 2006; Loick et al. 2007). Here, we present a comprehensive set of isotopic measurements of dissolved organic carbon, particulate organic carbon, particulate organic nitrogen, and mesozooplankton collected in the outer Amazon River plume in the context of hydrological, chemical, and biological measurements from the same cruise. A recent paper by Goes et al. (2014) described the phytoplankton biogeography of the Amazon plume system based on data collected during the same cruise, identifying three distinct communities, two of which are driven by N_2 fixation, either by "diatom-diazotroph" associations (DDAs), or by colonial cyanobacteria belonging to the genus *Trichodesmium* and unicellular *Synechococcus* spp. The third major phytoplankton community of Goes et al. (2014) is dominated by diatoms that lack diazotrophic symbionts. We test the hypothesis that the NGE of epipelagic mesozooplankton is highest at sites where N_2 is the principal new nitrogen source supporting primary production. We first identify and quantify the new nitrogen sources for the upper water column, then estimate and compare mesozooplankton NGE at three sites representative of the three distinct phytoplankton assemblages.

Materials and methods

Samples were collected during the R/V *Knorr* cruise KN197 (22 May 2010–22 June 2010) to the western tropical North Atlantic and outer Amazon River plume (Fig. 1; http://www.rvdata.us/catalog/KN197-08). A Seabird SBE-911 plus CTD-rosette system was used to measure hydrographic properties and collect water samples through the upper water column. Samples for inorganic nutrients (SiO_2, $NO_3 + NO_2$, and PO_4) were collected unfiltered from the rosette and analyzed at

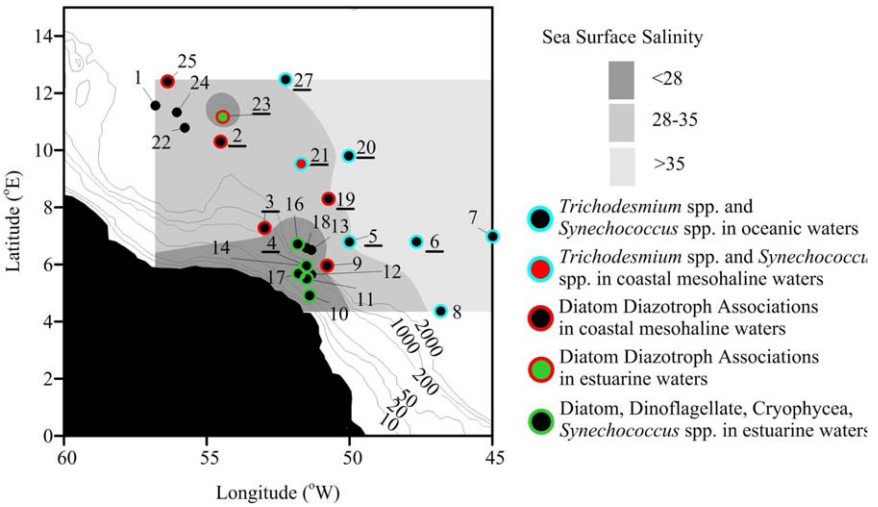

Fig. 1. Station map along the Amazon River Plume salinity gradient sampled in May 2010–June 2010. Stations selected are focused on those for which the dominant phytoplankton communities according to Goes et al. (2014) were identified as given in the color code. Station 6 and stations close to the shelf for which additional nutrient data was available (12 and 13) are also shown. Zooplankton isotopes were sampled during multiple tows at 10 stations (underlined).

sea using a Lachat QuikChem 8000 flow-injection analyzer, with an analytical precision for nitrate plus nitrite of ± 0.2 μmol L^{-1}. NH_4^+ concentration was measured at sea fluorometrically according to Taylor et al. (2007), with a precision of ± 0.02 μmol L^{-1}. Suspended particles were collected by gentle pressure filtration of 2–17 L of seawater through precombusted (450°C for 2 h) 47-mm GF/F filters that were dried at 60°C and stored over desiccant for analysis ashore. For isotopic analysis, filters containing particle samples were trimmed, and cut into quadrants or halves that were pelletized in tin capsules. Filters with uneven distribution of material were first ground to homogenize the sample, weighed, and subsampled for analysis.

Zooplankton were collected in oblique tows using a 1-m^2 Multiple Opening-Closing Net and Environmental Sensing System (MOCNESS; 202- μm mesh size) through the upper water column during the day and at night. Typically, the MOCNESS sampling depth intervals in the upper 100 m were: 0–25 m, 25–50 m, 50–100 m or 0–25 m, 25–50 m, 50–75 m, and 75–100 m. Zooplankton samples from each net were split with either a quarter or half of the sample preserved immediately in 4% buffered formaldehyde for taxonomic analysis. The remainder of the samples were size-fractionated using nested sieves with mesh sizes of 5000 μm, 2000 μm, 1000 μm, 500 μm, and 200 μm and then transferred onto preweighed disks of 200 μm Nitex mesh (Steinberg et al. 2012) for biomass and gut pigment measurements, and nitrogen and carbon elemental and isotopic analyses. All plankton size fractions were visually inspected for major taxa present using a stereo microscope (6–60X magnification) before being frozen (−20°C) at sea. Ashore, these samples were subsequently thawed and dried at 60°C for 24 h and weighed to determine biomass. The samples were then ground to a fine powder and subsampled for nitrogen and carbon elemental and isotopic analysis.

All natural abundance measurements of particulate and zooplankton nitrogen and carbon were made by continuous-flow isotope-ratio mass spectrometry (CF-IRMS) using a Micromass Optima interfaced to a CE NC2500 elemental analyzer. Particulate organic carbon (PC) samples for $\delta^{13}C$ analysis generally were not acidified, as calcifying organisms were not a significant component of the phytoplankton communities (E. J. Carpenter unpubl. data). All isotope abundances are expressed as $\delta^{15}N$ values relative to atmospheric N_2 and as $\delta^{13}C$ values relative to VPDB. Each analytical run included a size series of elemental (methionine) and isotopic (peptone) standards, which provided a check on stability of the instrument and allowed us to remove the contribution of any analytical blank from our isotopic measurements (Montoya 2008). In general our analytical blank was < 0.3 μmol C and < 0.15 μmol N. We conservatively estimate that the overall analytical precisions of our concentration and isotopic measurements are better than ± 0.15 μmol for nitrogen, ± 0.3 μmol for carbon, and $\pm 0.15‰$ for both $\delta^{15}N$ and $\delta^{13}C$.

We estimated mixed layer depths from the maximum in the buoyancy frequency of the water column (Turner 1980). The depth of the nitracline was taken as the shallowest depth where nitrate plus nitrite was found, and was compared to the vertical $\delta^{15}N$ PN structure associated with the nitrate uptake of phytoplankton (Montoya et al. 1992; Altabet 1996) to identify changes in the nitracline depth associated with the lateral advection of shelf waters along the flow of the river plume.

N_2 fixation rates were measured according to Montoya et al. (1996) using $^{15}N_2$ gas from Cambridge (98% $^{15}N_2$) with triplicate incubations in 4.6 L Nalgene bottles typically using water from six depths in the upper 100 m of the water

Table 1. Riverine and oceanic endmembers for the calculation of the conservative mixing line of $\delta^{13}C$ of dissolved organic carbon (DOC) and $\delta^{13}C$ particulate organic carbon (PC) along the Amazon River plume using the model described by Cai et al. (1988), and based on the DOC riverine endmember for $\delta^{13}C$ from Ellis et al. (2012), DOC concentration from Hedges et al. (1994), DOC oceanic endmembers from Medeiros et al. (2015), PC riverine endmembers from Cai et al. (1988), $\delta^{13}C$ PC oceanic endmember from Benner et al. (1997) and Schwamborn et al. (1999), and PC concentration and sea surface salinity (SSS) from this study.

	Riverine SSS = 0		Oceanic SSS = 35.8–36.3	
DOC	−29.3‰	371 μmol L^{-1}	−22.9‰	87 μmol L^{-1}
PC	−29.3‰	73 μmol L^{-1}	>−22.9‰	2.3 μmol L^{-1}

column. We note that our estimates of N_2 fixation may be conservative due to the time required for equilibration of $^{15}N_2$ gas with the incubation medium (Mohr et al. 2010; Dabundo et al. 2014). Dabundo et al. (2014) also caution that ^{15}N-ammonium contamination in $^{15}N_2$ gas from Cambridge may lead to an overestimation of N_2 fixation rates by 0.0008 nmol L^{-1} h^{-1}, but we had multiple experiments where ^{15}N incorporation into biomass was undetectable, especially at ES stations indicating minimal to nonexistent contamination by ^{15}N-ammonium or other bioavailable N species. Our experimental bottles were incubated under simulated in situ conditions for 24 h, then terminated by gentle pressure filtration (10–15 psi) onto precombusted GF/F filters after passage through a 10 μm prefilter. This filtration scheme produced large (> 10 μm) and small (< 10 μm) size fractions to separate N_2 fixation by unicellular and larger diazotrophs like DDAs or *Trichodesmium* (Agawin et al. 2014 and references therein). Areal N_2 fixation rates were calculated by trapezoidal integration from the surface to 100 m depth or to the seafloor, whichever was shallower.

Contributions of DOM

Samples collected during our cruise for measurement of DON concentrations were damaged during transport (P. L. Yager pers. comm.). We, therefore, use measurements of the concentration and $\delta^{13}C$ of DOC from the same cruise (Medeiros et al. 2015) to estimate the potential contribution of dissolved organic nitrogen to particles in our investigation area. Specifically, we used the relationship between sea surface salinity and the concentration and $\delta^{13}C$ of DOC to define the conservative mixing line for $\delta^{13}C$ DOC after Cai et al. (1988) using the endmember values in Table 1, then applied a literature value for the C: N ratio of Amazon DOM (Hedges et al. 1994) to estimate the potential nitrogen inputs to our study area via transport of DOM.

Quantification of diazotroph N in PN and zooplankton

We used the "concentration weighted" and depth-integrated $\delta^{15}N$ of PN (in the following termed $\delta^{15}N_{NCD}$) as a proxy for the isotopic composition of the base of the pelagic food web. We carried out a trapezoidal integration from the surface to the depth of the nitracline (Montoya et al. 1992) as follows:

$$\text{Weighted Mean } \delta^{15}N_{NCD} = \frac{\sum([PN]_i \times \Delta z_i \times \delta^{15}N_i)}{\sum([PN]_i \times \Delta z_i)} \quad (1)$$

where $[PN]_i$ represents the particulate nitrogen concentration (μmol L^{-1}), $\delta^{15}N_i$ represents the isotopic composition of suspended particles, and Δz_i is the depth interval (m) represented by sample i. The individual layers, of thickness Δz, were bounded by the midpoints between sample depths, and the integration extended from the surface to the nutricline depth. At stations that showed changes in water masses during extended PN and zooplankton sampling (Stas. 2, 6, 19, 20, 23, 25, and 27, see Supporting Information Fig. S1 for water mass analysis), we used the PN profile from the CTD cast that was nearest in time to the MOCNESS tow for comparison to zooplankton.

We used zooplankton from the 0–25 m and the 25–50 m depth strata to estimate the contribution of diazotroph N to the planktonic food web. This approach should minimize the potential impact of isotopically enriched particles from below the nitracline, providing a robust estimate of the inputs of diazotroph N in the surface mixed layer (Altabet 1989; Landrum et al. 2011).

The diazotroph N contribution was calculated for both particles and mesozooplankton using the isotope mass balance approach of Montoya et al. (2002). The contribution of diazotroph nitrogen to suspended particles was calculated as:

$$\%\ \text{Diazotroph } N = 100 \times \left(\frac{\delta^{15}N_{NCD} - \delta^{15}N_{Nitrate}}{\delta^{15}N_{Diazo} - \delta^{15}N_{Nitrate}}\right) \quad (2)$$

where $\delta^{15}N_{NCD}$ is the weighted mean $\delta^{15}N_{PN}$ of PN calculated using Eq. 1, $\delta^{15}N_{Nitrate}$ is the isotopic endmember of 4.5‰ for deep-water nitrate (Knapp et al. 2008), and $\delta^{15}N_{Diazo}$ is the isotopic endmember of −2‰ for N_2 fixation into particles (Montoya et al. 2002).

The contribution of diazotroph nitrogen to mesozooplankton biomass was calculated as:

$$\%\,\text{Diazotroph } N = 100 \times \left(\frac{\delta^{15}N_{Zoo} - \delta^{15}N_{Reference\ Zoo}}{\delta^{15}N_{Diazo} - \delta^{15}N_{Reference\ Zoo}}\right) \quad (3)$$

where $\delta^{15}N_{Zoo}$ is the $\delta^{15}N$ value of one of the five zooplankton size fractions collected from each depth interval sampled, $\delta^{15}N_{Diazo}$ is the isotopic endmember of −2‰ for diazotrophic N, and $\delta^{15}N_{Reference\ Zoo}$ is a reference $\delta^{15}N$ for zooplankton collected in regions not heavily influenced by

consumption of diazotroph nitrogen as described by Landrum et al. (2011). These reference values provide an index to the scaling of δ^{15}N with animal size, and the low reference values we used provide a conservative estimate of the diazotroph contribution to biomass.

Estimation of the nitrogen specific net growth efficiency

We used an open system Rayleigh fractionation model for the steady state case where the amount of N incorporated through feeding is equal to the amount of N lost through excretion as described by Montoya (2007). We are focusing on the steady state by minimizing the impact of the natural temporal variability in δ^{15}N by eliminating all stations with evidence for recent changes in δ^{15}N and estimated NGE only for stations where the observed variability of the δ^{15}N PN values above the nitracline and the zooplankton δ^{15}N values from the 0–25 m and the 25–50 m depth strata was $< 1‰$. At steady state, we then look at the partitioning of isotopes required to produce the enrichment in ^{15}N we observe in the zooplankton size fractions under the assumption that excretion is the only process that significantly affects the $\Delta\delta^{15}$N that we measured:

$$\delta^{15}N_{Zoo} = \delta^{15}N_{NCD} - \varepsilon \times \ln f \quad (4)$$

where $\delta^{15}N_{Zoo}$ is the δ^{15}N value of the smallest zooplankton size fraction (200–500 μm) in a specific depth stratum (50–25 m or 25–0 m), ε is the isotopic enrichment factor of $-2.7‰$ for NH_4^+ excretion by zooplankton (Checkley and Miller 1989), and $\delta^{15}N_{NCD}$ is the weighted mean δ^{15}N of PN between the surface and the nitracline (Eq. 1). Equation 4 can be rearranged to yield an expression for f, the fraction of assimilated nitrogen remaining in the animal's body:

$$f = \exp\left(\frac{\delta^{15}N_{NCD} - \delta^{15}N_{Zoo}}{\varepsilon}\right) \quad (5)$$

which is equivalent to the NGE of the animal. Using a value of $\varepsilon = -2.7‰$ and an isotopic difference ($\Delta\delta^{15}N = \delta^{15}N_{NCD} - \delta^{15}N_{Zoo}$) of 3‰, for example, implies a NGE of 0.33% or 33%. Note that the substrate pool for deamination and excretion in an actively feeding animal would be weighted toward the food consumed. Under these conditions, an animal will release NH_4^+ with a δ^{15}N lower than that of the food consumed and more than 2.7‰ lower than the δ^{15}N of the animaĺs tissues (Frazer et al. 1997). Therefore, this simple approach provides an upper limit for the overall efficiency of transfer of nitrogen through the food web to a particular size fraction of zooplankton (Montoya 2007). For more complex situations with time-varying diet, we refer to the Ramesh–Singh model (Ramesh and Singh 2010).

For larger zooplankton (size fractions > 500 μm), we used the slopes of the linear regressions of $\delta^{15}N_{Zoo}$ as a function of size as an index to N transfer efficiency among the different zooplankton size fractions from the upper 50 m as in Montoya et al. (2002).

Results

Goes et al. (2014) identified three distinct phytoplankton communities separated largely on the basis of salinity gradients across the plume (Fig. 1). These three assemblages included an Estuarine Type (ES) Community located upstream of the plume on the shelf at salinities below 28 and comprised of a high biomass mixed population of diatoms, dinoflagellates, cryptophytes, and green-water *Synechococcus* spp. A second, coastal Mesohaline (MH) Community was located in the northwestern region of the plume off the shelf at salinities between 28 and 35 and contained abundant Diatom-Diazotroph Associations (DDAs, mostly *Hemiaulus* sp./*Richelia* sp.). The third, Oceanic (OC) Community was dominated by *Trichodesmium* spp. and oceanic *Synechococcus* spp. in the oligotrophic offshore waters outside of the plume with salinities above 35. DDAs, *Trichodesmium* spp., and *Synechococcus* spp. are all capable of N_2 fixation (Mitsui et al. 1986; Carpenter and Capone 2008), while the dominant phytoplankton in the Estuarine Type Community must rely on other N sources for growth. We additionally separated the MH community into two subgroups, MH1 and MH2. These two MH groups differed in multiple ways, including their nutrient concentrations (MH1 > MH2, Table 2), DDA cell abundance at the surface (MH1 $\ll$ MH2), and the relatively low abundances or absence of asymbiotic diatoms at MH2 stations (Goes et al. 2014). Station 23 was unique in that it was the only station with moderate DDA abundances and high N_2 fixation rates despite having low salinity comparable to shelf waters at ES stations, and, therefore, is listed separately in Table 2. Station 21 had a sea surface salinity below 35 (33.6) but was dominated by *Trichodesmium* spp. and oceanic *Synechococcus* spp. according to Goes et al. (2014), and therefore was also listed separately in Table 2. Station 6 was not included in the study of Goes et al. (2014) but was characteristic of an OC station (Table 2), including dominance by *Trichodesmium* spp. (R. A. Foster unpubl. data) and, therefore, classified as an OC station. Stations 12 and 13 were not classified by Goes et al. (2014) but nutrient data for these two shelf stations were added for a higher resolution of nutrient distribution at ES stations (Figs. 3, 4).

Nitrogen sources from the river, subsurface waters, and N_2 fixation

The mixed layer and nitracline depths were shallowest at the ES stations on the shelf and deepest at the OC stations (Table 2; Figs. 2A,B). Surface waters (2–10 m) generally were depleted in dissolved inorganic nitrogen (DIN: nitrate, nitrite, ammonium), except at ES Stas. 4, 10, 12, 17 (Fig. 3A), and MH1 Sta. 9 (Fig. 3B), where the nitracline shoaled into surface waters (Figs. 2A, 4A). The nitracline depth was 20 m or shallower at ES Stations, 20 m at MH1 Sta. 3 and in four

Table 2. Summary of physical and chemical properties (mean ± SD) for the phytoplankton communities identified by Goes et al. (2014) with a subdivision of the mesohaline community into MH1 and MH2, and Stats. 21 and 23 displayed separately. See text for further details.

	Estuarine	Mesohaline 1	Mesohaline 2	Oceanic	Sta. 21	Sta. 23
Stations	4, 10, 11, 14, 16, 17	3, 9	2, 19, 25	5, 6, 7, 8, 20, 27		
mixed layer depth (m)	6 ± 1	11.0 ± 0	20.0 ± 8	37 ± 16	17	8
depth of the nitracline (m)	10 ± 10	23 ± 4	68 ± 35	88 ± 14	80 (10*)	100 (24*)
sea surface salinity	20.9 ± 2.0	31.3 ± 0.2	33.0 ± 1.5	35.5 ± 0.3	33.6	26.2
surface silicate (μmol L^{-1})	42.3 ± 8.5	19.3 ± 3.2	4.1 ± 1.7	1.3 ± 0.8	5.75	26.3
surface phosphate (μmol L^{-1})	0.39 ± 0.08	0.24 ± 0.06	0.05 ± 0.05	0.08 ± 0.09	0.12	0.37
surface nitrate+nitrite (μmol L^{-1})	0.16 ± 0.26†	0.00 ± 0.00	0.00 ± 0.00	0.00 ± 0.00	0.00	0.00 ± 0.00
NH_4^+100m (μmol L^{-1})	0.06 ± 0.09†	0.31 ± 0.41	0.23 ± 0.14	0.04 ± 0.06	0.01	0.46
areal N_2 fixation (μmol m^{-2} d^{-1})	21 ± 17†	70 ± 50	181 ± 122	98 ± 49	73	186 ± 57
$\delta^{15}N_{NCD}$ (‰)	3.6 ± 1.0	2.6 ± 0.8	−1.7 ± 1.7	−1.6 ± 1.7	2.8 ± 0.8*	2.8 ± 0.6*

*corrected nitracline depths for Sta. 21 and Sta. 23 as identified from the δ^{15}N PN depth profiles, see text for more details.
†no data for Sta. 16.

out of five profiles at Sta. 9, and 50 m or greater at most MH2 and OC stations, except for MH2 Sta. 25, where at times nitracline depth was 30 m (Fig. 4).

At most stations, the nitracline was accompanied by a shift in δ^{15}N PN values (Figs. 4, 8) consistent with isotopic fractionation during uptake of nitrate by phytoplankton (see below). Noteworthy features at Stas. 21 and 23 were deep nitraclines (at 80 m and 100 m, respectively) with δ^{15}N PN profiles that suggest previous nitrate injections at 10 m and 22–25 m, respectively (Supporting Information Table 1). These features occurred at depths comparable to the shallow nitraclines observed at ES and MH1 stations.

In contrast to DIN, surface phosphate and silicate concentrations show a clear impact of low salinity waters from the river plume, indicating that phosphate was entering surface waters from both riverine and subsurface sources (Fig. 3B), while silicate was supplied primarily by riverine waters (Fig. 3C).

Enhanced N_2 fixation rates (> 0.1 nmol L^{-1} h^{-1}) were found in all phytoplankton communities but mainly in the upper 50 m of the water column at MH1, MH2, and OC stations, with a maximum rate of 0.55 nmol L^{-1} h^{-1} at MH2 Sta. 25 (Fig. 5). We did not find any trends in the size distribution (< 10 μm and > 10 μm) of active diazotrophs in any community although it is interesting to note that we found enhanced N_2 fixation rates in the >10 μm size fraction at two ES stations (Stas. 4 and 16, Table 3). Total areal N_2 fixation rates were highest at MH2 stations (181 ±122 μmol m^{-2} d^{-1}), followed by OC stations including Sta. 21 and MH1 stations including Sta. 23 (110 ± 53 μmol m^{-2} d^{-1} and 99 ± 71 μmol m^{-2} d^{-1}, respectively). The lowest mean areal rates (21 ± 17 μmol m^{-2} d^{-1}) were found at ES stations (Table 3).

Ammonium concentrations were low at most ES and OC stations but were clearly enhanced at MH1 and MH2 stations (Fig. 6). The vertical position of the maximum ammonium concentration coincided with the position of the nitracline at Stas. 2, 19, and 25 although elevated concentrations occurred both above and below the nitracline at these stations. A noticeable exception was Sta. 23, where high ammonium concentrations (0.3–1.2 μmol L^{-1}) occurred above the nitracline depths.

Distributions of δ^{13}C DOC and δ^{13}C PC

The δ^{13}C of DOC closely followed the conservative mixing line between riverine and oceanic DOC, while the δ^{13}C of PC was higher than the values for riverine influenced DOC with two outliers at Stas. 5 and 21 (Fig. 7). Dissolved organic carbon concentrations were highest in low salinity estuarine waters and decreased toward oceanic waters (Supporting Information Fig. S2A). In contrast, particulate organic carbon (PC) and nitrogen (PN) concentrations showed no correlation with salinity (Supporting Information Fig. S2B,S2C) and were mainly low with average PN concentrations of 0.8 ± 0.6 μmol L^{-1} (n = 79, Supporting Information Fig. S2C).

ES station properties (Stas. 4, 10, 11, 14, 16, 17)

Estuarine stations were characterized by low sea surface salinity (SSS; 17.0-26.2) and high abundances of non-diazotrophic phytoplankton (Goes et al. 2014). The biomass and depth-weighted mean $\delta^{15}N_{NCD}$ was highest at ES stations with an average of 3.6 ± 1.0‰ (Table 2). The δ^{15}N of PN varied between 3‰ and 5‰ in the upper 10 m and patterns varied with depth. For example, the δ^{15}N of PN rapidly decreased with depth to −6‰ at Sta. 4, but was comparatively invariant with depth at Stas. 10, 11, 14, and 17 (mean ± SD = 4.5 ± 0.9‰).

The δ^{15}N of zooplankton in the upper 50 m at Sta. 4 varied around a mean of 4.5 ± 0.8‰ in the two smaller size fractions, and was higher in the three larger size fractions with a

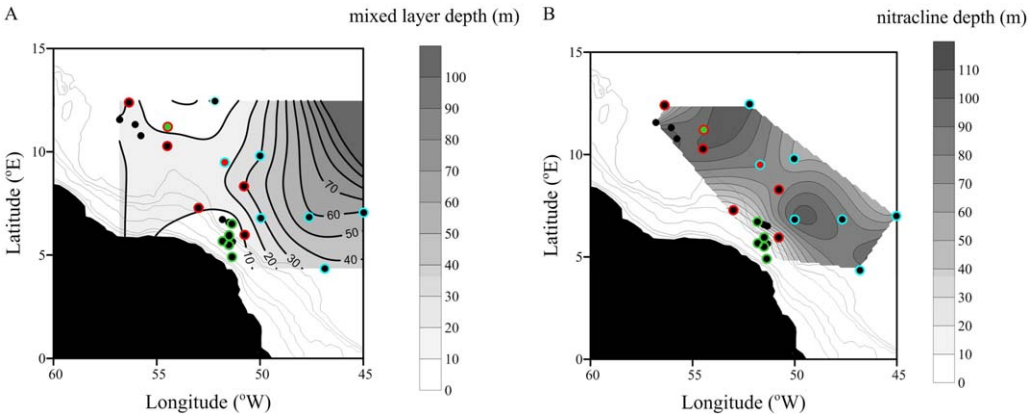

Fig. 2. (A) Mixed layer depth (m), and (B) depths of the nitracline (m). At representative stations, the phytoplankton community as identified by Goes et al. (2014) is superimposed according to the color code in Fig. 1.

mean value of $5.9 \pm 0.5‰$ (Figs. 9A1,A2). Within a depth interval, the $\delta^{15}N$ of zooplankton either increased significantly or insignificantly with animal size (see Supporting Information Table 2 for individual p and r^2 values), with an isotopic spread of $4.1‰$ to $6.5‰$ across size fractions (Fig. 9A1), though the largest size fraction (> 5000 μm) sometimes had particularly low $\delta^{15}N$ values (Fig. 9A2, Supporting Information Table 2). For example, one very low $\delta^{15}N$ value ($1‰$) was found in the largest size fraction (> 5000 μm) in the upper 25 m of the water column (Fig. 9A2).

MH station properties (MH1 Stas. 3, 9, 23; MH2 Stas. 2, 19, 25)

The Mesohaline stations were characterized by high abundances of DDAs capable of N_2 fixation and intermediate SSS (31.1-34.8), except for Sta. 23, where enhanced DDA as well as *Synechococcus* spp. abundances were found despite a low salinity of 26.2 (Goes et al. 2014). The depth weighted $\delta^{15}N_{NCD}$ values at MH stations showed two patterns, with MH1 stations and Sta. 23 being similar to the ES stations with an average of $2.6 \pm 0.8‰$ and $2.8 \pm 0.6‰$, respectively, while the average value for MH2 stations was the lowest among all communities at $-1.7 \pm 1.7‰$ (Table 2). The $\delta^{15}N$ of surface PN was highly variable and ranged from $-5.0‰$ to $3.7‰$ (Fig. 8B1–B3). The $\delta^{15}N$ of PN above the nitracline was also highly variable. For example, $\delta^{15}N$ of PN at Sta. 2 decreased markedly from $-2.7‰$ in surface waters to $-11.0‰$ at 60 m depth. In contrast, the profiles at Sta. 19 were comparatively invariant around a value of $-0.5 \pm 0.3‰$. At Stas. 9 and 23, either a clear minimum (Sta. 23) or a clear maximum (Sta. 9) was found at 30 m to 40 m depth. At Sta. 9, the maximum coincided with the nitracline at 30 m depth, but at Sta. 23, the minimum occurred at 40 m, well above the depth of the nitracline at 100 m (Supporting Information Table 2). Two CTD casts taken 4 h apart at Sta. 3 showed a similar contrast between a local maximum and minimum at the nitracline depth of 20 m (Fig. 8B1). Similarly, $\delta^{15}N$ PN changed at the nitracline depth of 30 m from $-0.3‰$ to $8.7‰$ within 2 h of sampling at Sta. 25 (Fig. 8B3).

Zooplankton in the two smallest size fractions at MH stations also fell into two groups, with a mean $\delta^{15}N$ of $1.5 \pm 0.6‰$ at MH2 Stas. 2 and 19 and a higher mean $\delta^{15}N$ of $4.9 \pm 1.0‰$ at MH1 Stas. 3 and 23 (excluding one very high outlier at 25–50 m depth). The $\delta^{15}N$ values of the larger zooplankton size fractions (> 1000 μm) were more similar at the MH1 and MH2 stations. Like the $\delta^{15}N$ of PN (Fig. 8), the $\delta^{15}N$ of zooplankton at MH1 Stas. 3 and 23 was more variable than at MH2 Stas. 2 and 19 (mean values of $5.0 \pm 1.7‰$ and $2.3 \pm 0.9‰$, respectively), with very high ($7.3‰$ to $10.4‰$) or very low ($-2.8‰$) outliers, especially in the larger size fractions (Fig. 9). Due to water mass changes (Supporting Information Fig. S1), the PN profiles closest in time to the MOCNESS tows were used for the PN-zooplankton comparisons at Stas. 19 and 23.

Zooplankton at MH1 stations showed no significant correlation in $\delta^{15}N$ with size. At some stations, $\delta^{15}N$ increased slightly with animal size (Fig. 9B1), while the two MH1 stations showed an overall negative trend in $\delta^{15}N$ with animal size due to low ($3.7‰$) and very low $\delta^{15}N$ ($-2.8‰$) values in the largest size fraction (Fig. 9B2, Supporting Information Table 2). At one of the MH2 stations, zooplankton showed a highly significant positive relationship between $\delta^{15}N$ and size, while the $\delta^{15}N$ of zooplankton at the other MH2 station did not vary significantly with size (Fig. 9C1,C2, Supporting Information Table 2).

OC station properties (Stas. 5, 6, 7, 8, 20, 21, 27)

The Oceanic stations were mainly characterized by high sea surface salinity (SSS, >35), except for Sta. 21 with a SSS of 33.6 (Table 2), and by high abundances of *Trichodesmium* spp. and oceanic *Synechococcus* spp. (Goes et al. 2014). The $\delta^{15}N$ of surface particulate nitrogen at OC stations ranged from $-6.1‰$ to $2.1‰$ (Figs. 8C1–C3), with mean depth weighted $\delta^{15}N_{NCD}$ at OC stations (excluding Sta. 21) of $-1.6 \pm 1.7‰$, which was close to the MH2 values (Table 2).

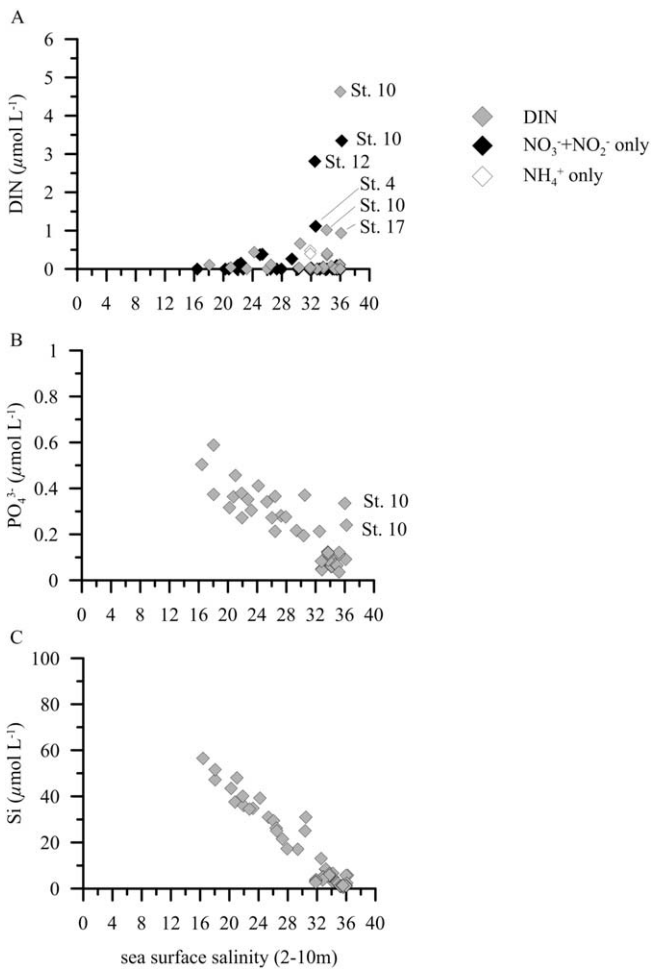

Fig. 3. Sea surface salinity (2–10 m) vs. sea surface (2–10 m) nutrient distribution in μmol L^{-1} of (A) dissolved inorganic nitrogen (DIN) including nitrate, nitrite, and ammonium, (B) phosphate, and (C) silicate concentrations. Individual ES stations with high DIN concentrations at the oceanic endmember salinity are indicated.

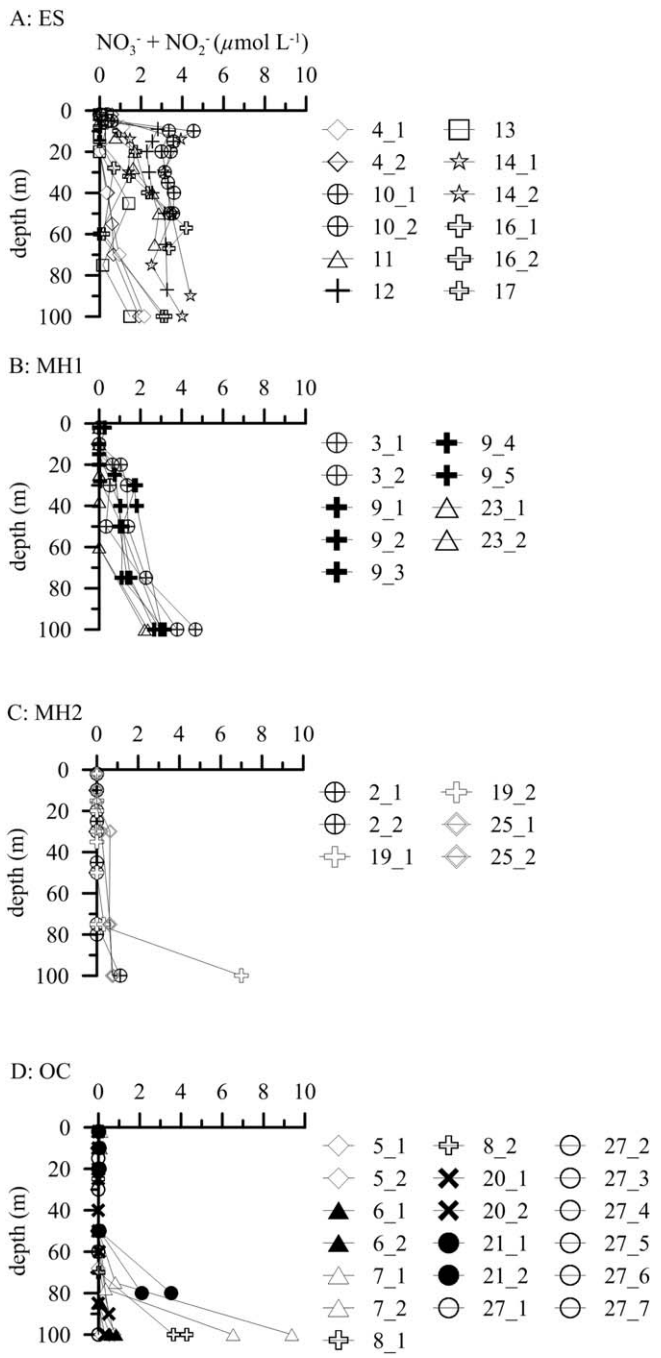

Fig. 4. Vertical profiles of the nitrate (NO_3^-) plus nitrite (NO_2^-) concentrations from multiple casts from stations classified into phytoplankton communities along the plume salinity gradient (see Fig. 1). ES, estuarine; MH1 and MH2, subdivisions of the mesohaline community; OC, oceanic. Stations with replicate profiles are indicated.

The $\delta^{15}N$ of PN was highly variable with depth at most OC stations, with surface values ranging from $-6.4‰$ to $2.3‰$ (Figs. 8C1–9C3). In contrast, individual profiles at Stas. 7 and 27 varied little with depth (Figs. 8C1–C3). Due to water mass changes (Supporting Information Fig. S1), the PN profiles closest in time to the MOCNESS tows were used for the PN-zooplankton comparisons at Stas. 20, and 27.

Zooplankton in the two smallest size fractions at OC Stas. 20 and 27 had low $\delta^{15}N$ values of $0.9 \pm 0.3‰$, while animals from these size fractions at Stas. 5, 6, and 21 had a higher mean of $2.6 \pm 0.8‰$ (Fig. 9D1,D2). The two largest size fractions of zooplankton at the OC stations showed greater variation in $\delta^{15}N$ with depth than the smaller size fractions, with frequent outliers of considerably higher or lower $\delta^{15}N$ (Supporting Information Fig. S3L and S3K). At Sta. 20 and in some depth intervals from Stas. 5 and 27, we found a significantly positive relationship between zooplankton $\delta^{15}N$ and animal size (Fig. 9D1, Supporting Information Table 2), while most of the time there was no correlation between $\delta^{15}N$ and animal size due to low and very low $\delta^{15}N$ values in the largest zooplankton size fraction (Fig. 9D2, Supporting Information Table 2).

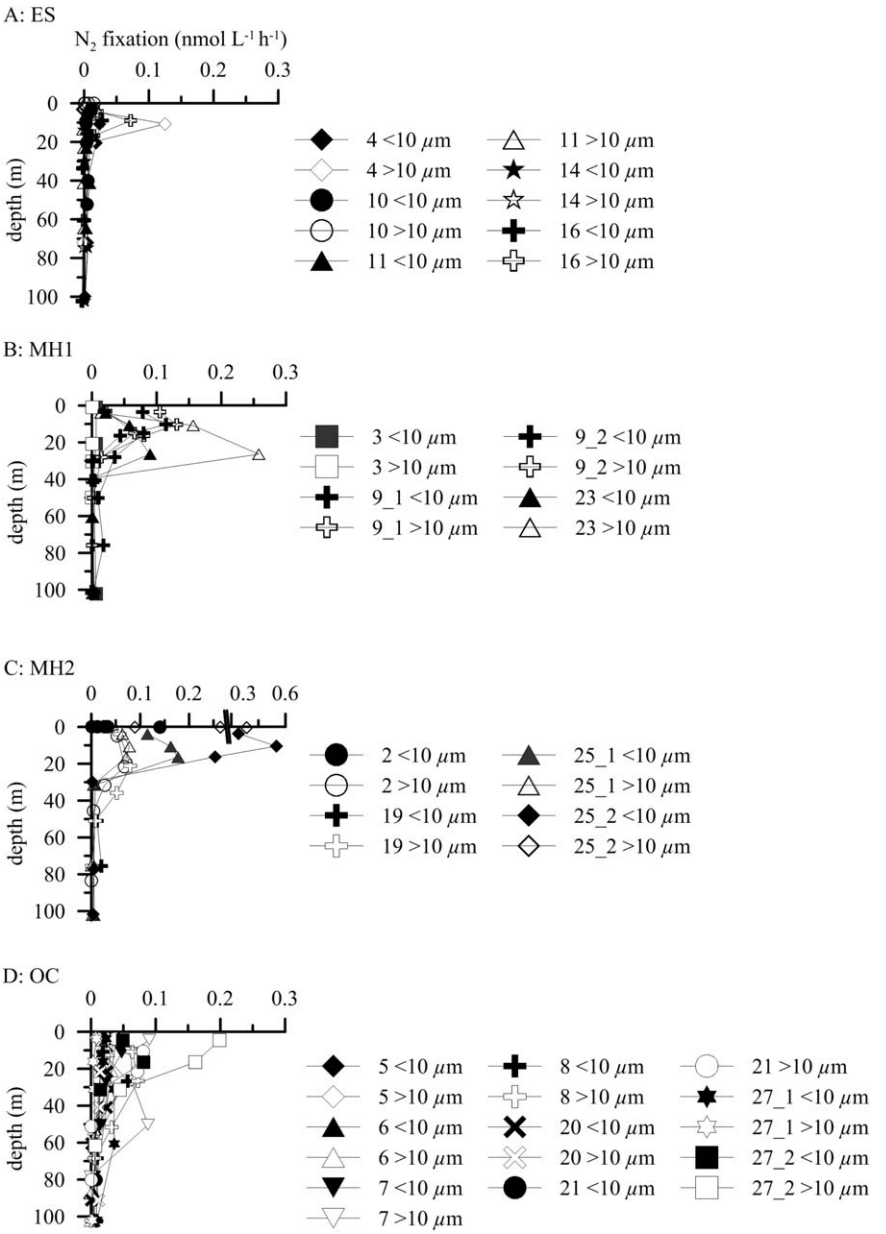

Fig. 5. Vertical profiles of nitrogen fixation rates (nmol L^{-1} h^{-1}) in large (>10 μm) and small (<10 μm) size fractions from stations classified into the phytoplankton communities along the plume salinity gradient (see Fig. 1). ES, estuarine; MH1 and MH2, subdivisions of the mesohaline community; OC, oceanic. Note the axis break in panel 5C.

Diazotroph nitrogen in PN and zooplankton

The amount of diazotroph nitrogen in PN and zooplankton was estimated with an isotopic mixing model. The PN estimate focused on the mixed layer, which was defined using the nitracline depth at all stations except for Stas. 21 and 23, where we used a shallower depth of integration (10 m and 22–25 m, respectively) based on the structure of the δ ^{15}N-PN profiles (Supporting Information Table 1).

The contribution of diazotroph nitrogen relative to subthermocline nitrate to PN in the upper water column above the nitracline was lowest at ES stations (mean ± SD = 13 ± 15%), intermediate at MH 1 stations including Sta. 23 (mean ± SD = 28 ± 11%), and highest at MH2 (mean = 86 ± 12%) and OC stations including Sta. 21 (mean ± SD = 79 ± 24%, Table 4). This trend was also apparent in the zooplankton (Table 4). At MH2 and OC stations, the diazotroph contribution to zooplankton N tended to decrease with animal size, while at ES and MH1 stations only the larger size fractions (> 1000 μm) showed measurable contributions of diazotroph N (Table 4).

Table 3. Areal daily N_2 fixation rates (μmol m^{-2} d^{-1}) in the size fractions <10 μm, >10 μm, and total at the individual stations and the phytoplankton communities (mean ± SD) as identified by Goes et al. (2014) with a subdivision of the mesohaline community into MH1 and MH2, and Stas. 21 and 23 included into OC and MH1, respectively.

	Sta.	<10 μm	>10 μm	Total
Estuarine	4	19	29	48
	10	7	2	9
	11	8	2	10
	14	8	3	11
	16	10	19	28
Mesohaline 1	3	12	1	13
	9	53 ± 10, *n*=2	46 ± 20, *n*=2	99 ± 10, *n*=2-
	23	53	134	187
Mesohaline 2	2	71	50	121
	19	24	71	95
	25	153 ± 75, *n*=2	100 ± 79, *n*=2	253 ± 154, *n*=2
Oceanic	5	28	14	42
	6	24	31	55
	7	42	117	159
	8	47	75	121
	20	35	31	67
	21	14	60	73
	27	67 ± 13, *n*=2	73 ± 83, *n*=2	141 ± 70, *n*=2
ES		10 ± 5	11 ± 12	21 ± 17
*MH*1 incl. Sta. 23		42 ± 21	57 ± 57	99 ± 71
*MH*2		100 ± 77	80 ± 52	181 ± 122
OC incl. Sta. 21		40 ± 20	59 ± 46	110 ± 53

NGE of zooplankton

We calculated the NGE for zooplankton from Stas. 19, 20, 21, 23, and 27, where both the δ^{15}N of PN above the nitracline and of zooplankton from the 0–25 m and the 25–50 m depth strata showed < 1‰ variation. This approach minimized the potential impact of transient and spatial variation on the isotopic difference between consumer and diet pairs. As we did for the diazotroph N calculations, we used the nitracline depth (Fig. 4) as a lower bound for NGE calculations for Stas. 19, 20, and 27, while for Stas. 21 and 23, we used a shallower depth based on the structure of the δ^{15}N PN profiles (Supporting Information Table 1). The resulting isotopic difference between the biomass and depth-weighted mean δ^{15}N of PN ($\delta^{15}N_{NCD}$) and the δ^{15}N of the smallest zooplankton size fraction (200–500 μm) was 1.6 ± 0.9‰ (Supporting Information Fig. S4). This mean isotopic difference between PN and zooplankton implies a NGE of 59% ± 10%.

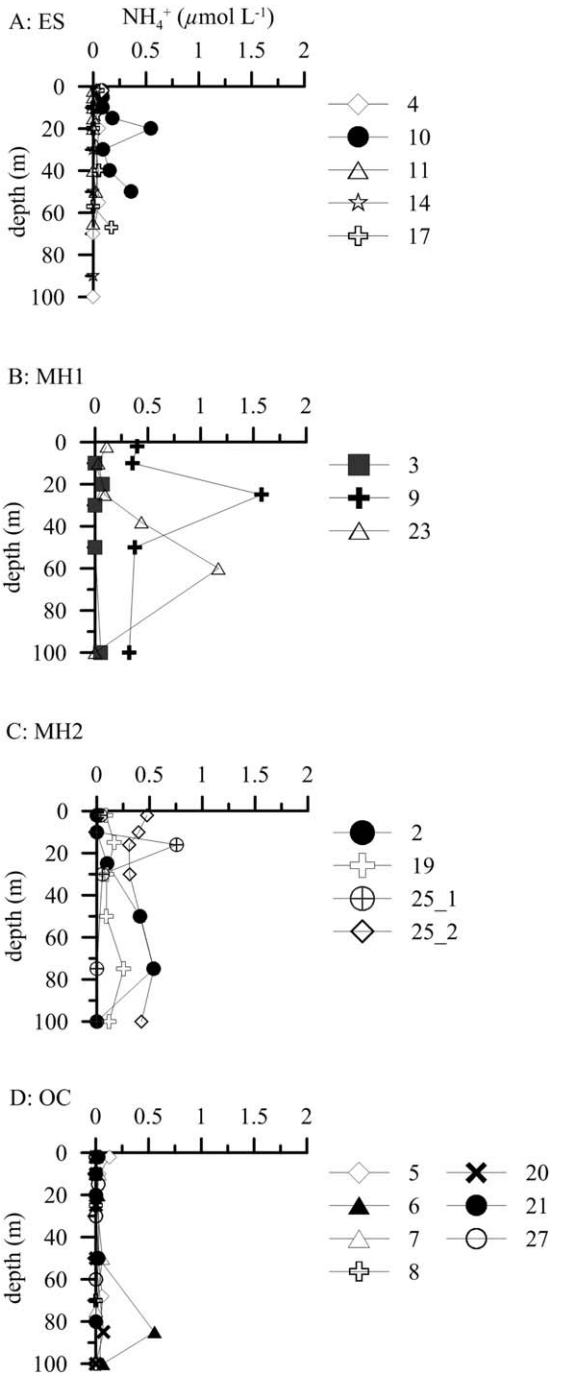

Fig. 6. Vertical profiles of ammonium concentrations (μmol L^{-1}) from stations classified into the phytoplankton communities along the plume salinity gradient (see Fig. 1). ES, estuarine; MH1 and MH2, subdivisions of the mesohaline community; OC, oceanic. Replicate profiles for Sta. 25 are indicated.

Surprisingly, we found no spatial differences in NGE among stations (Fig. 10).

The transfer efficiency of nitrogen was assessed qualitatively for larger zooplankton in the upper 50 m of the water column for all 10 stations sampled (Fig.1). Very shallow

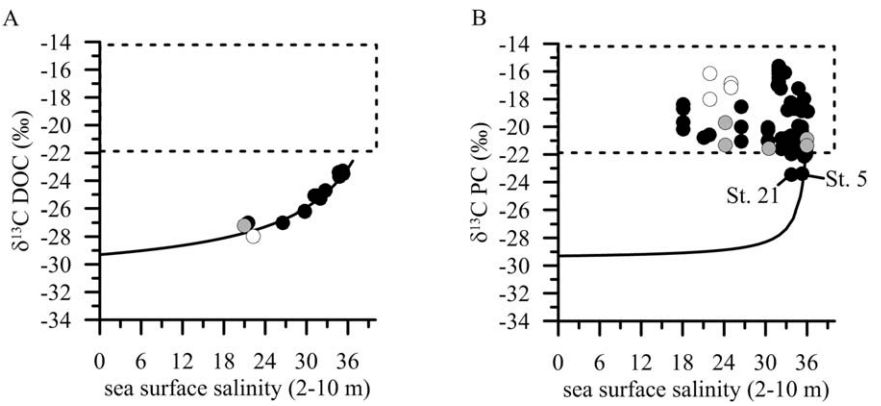

Fig. 7. (A) Surface salinity (2–10 m) vs. the δ^{13}C PC (in ‰) including the conservative mixing line after Cai et al. (1988), using the endmembers described in the text. (B) Surface salinity (2–20 m) vs. δ^{13}C DOC (in ‰) from Medeiros et al. (2015) including the conservative mixing line after Cai et al. (1988), using the endmembers from Table 1. ES Stas. 4 and 10 are white and gray, respectively. Single δ^{13}C PC values from oceanic Stas. 5 and 21 are indicated due to their close proximity to the conservative mixing line of δ^{13}C DOC. Square field indicates typical oceanic phytoplankton endmember δ^{13}C PC values as explained in the text.

(slope < 0.1) or negative slopes due to low δ^{15}N values in the two largest size fractions (2000–5000 μm and > 5000 μm) occurred frequently at stations from ES, MH1, and OC communities, while at MH2 stations the minimum slope was 0.4 (Fig. 9A2–D2, Supporting Information Table 2). We found phytoplankton contamination only in the two smallest size

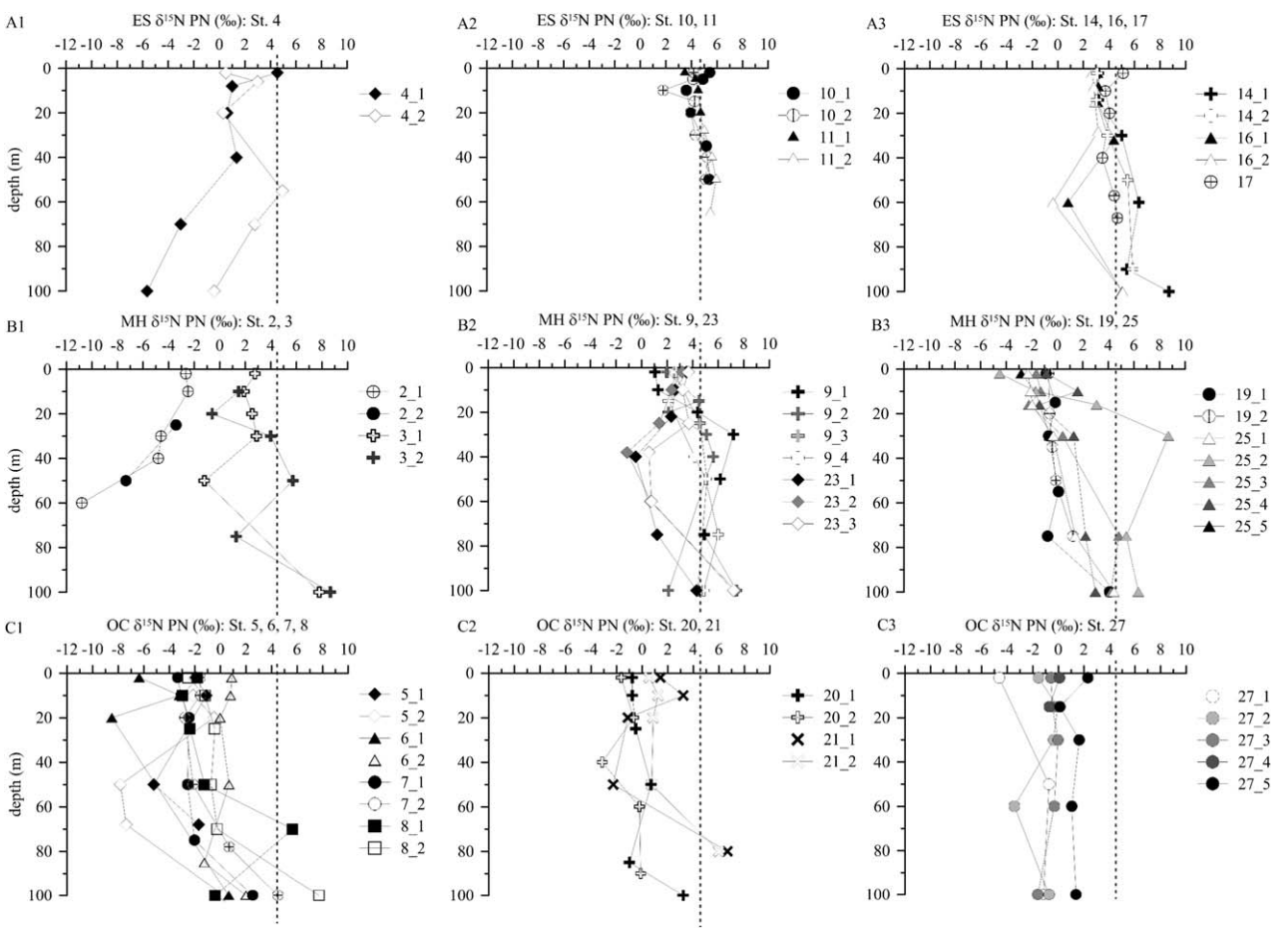

Fig. 8. Vertical δ^{15}N profiles (‰) of PN from (upper panel) Estuarine Stations (ES), (mid panel) Mesohaline Stations (MH), and (lower panel) Oceanic Stations (OC). Vertical dashed lines indicate the typical deep nitrate δ^{15}N values of 4.5‰.

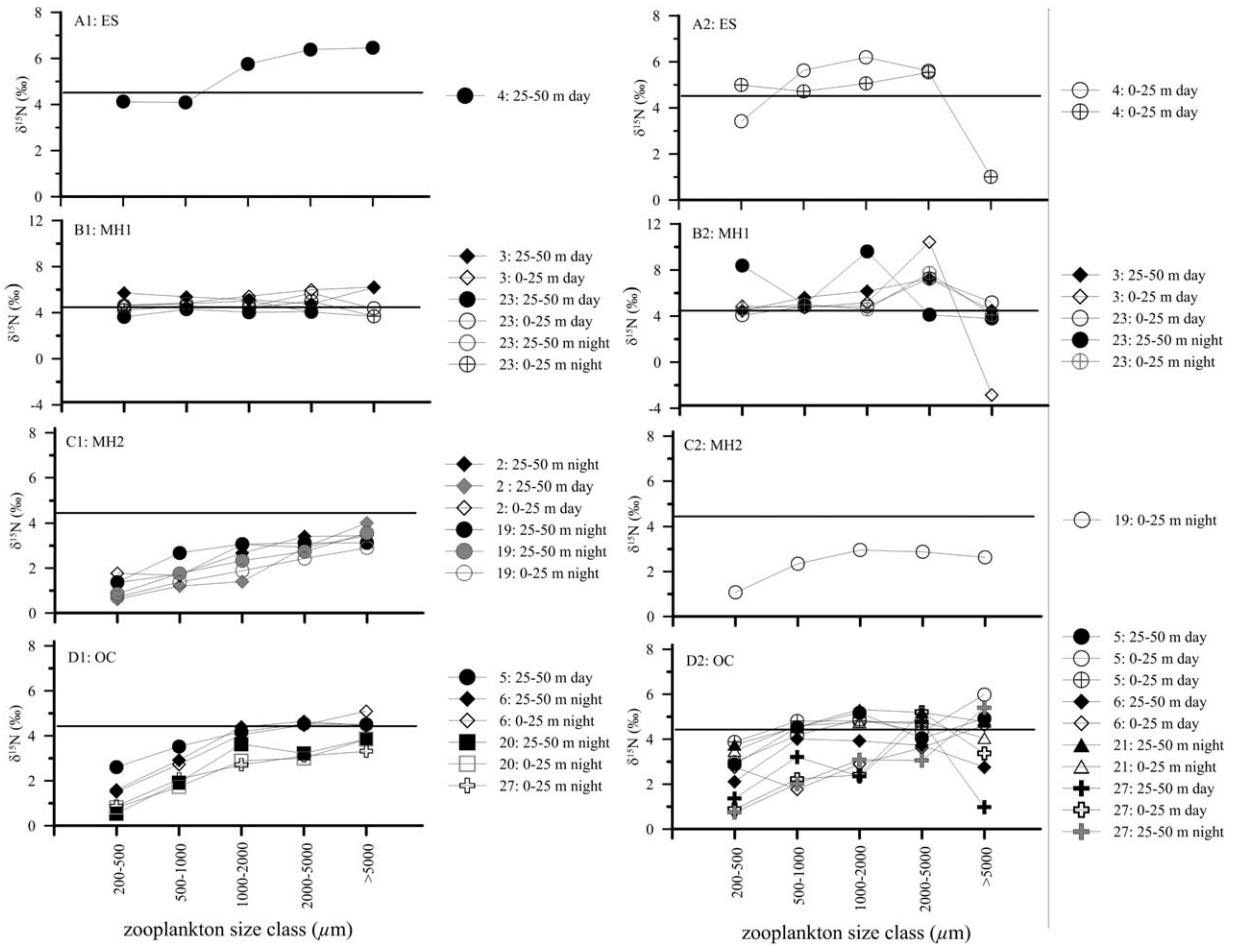

Fig. 9. δ^{15}N of zooplankton as a function of size fraction at ES, Estuarine Stations (A1 and A2); MH1 (B1 and B2) and MH2 (C1 and C2), subdivisions of the Mesohaline Stations; and OC, Oceanic Stations (D1 and D2). The solid horizontal line in each panel represents a typical δ^{15}N for deep-water nitrate.

fractions at Sta. 23, so some other factor must account for the low δ^{15}N values in the larger size fractions. Despite these qualitative differences, we found no statistically significant differences among the slopes for zooplankton from the different stations (one-way ANOVA, Supporting Information Table 3).

Discussion

The relatively few studies to date that have explored the NGE of zooplankton indicate a clear divergence between nearly constant NGE values measured in controlled laboratory experiments (summarized by Touratier et al. 1999) and variable NGE estimates from field measurements (Le Borgne 1982 and references therein). This discrepancy contributes to large uncertainties regarding the role of zooplankton in biogeochemical cycles (Anderson et al. 2013). Our stable nitrogen isotope approach (Montoya 2007) provides a robust, "time integrated" estimate of the NGEs of mesozooplankton (200–500 μm) from the outer Amazon River plume and adjacent oceanic waters. Interestingly, our data showed no correlation between mesozooplankton NGE and the contribution of diazotroph nitrogen to particles, food quality as reflected in PN: PC ratios, or food quantity as measured by PN and Chl *a* concentrations (not shown). Our findings thus corroborate earlier suggestions from laboratory experiments and modeling exercises that mesozooplankton may adjust their feeding behavior in response to changes in food quality and quantity in order to maintain constant nitrogen specific net growth efficiencies and elemental (C: N) ratios in their tissues.

Nutrient sources from the river, subsurface waters, and N_2 fixation

The discharge of the Amazon River forms a spatially heterogeneous surface plume extending more than 3000 km across the western tropical North Atlantic in summer and fall (Lentz 1995; Coles et al. 2013). During the period of highest discharge in April–May, the plume extends northward along the South American coast (Demaster and Pope

Table 4. Estimated contribution of N_2 fixation (mean ± SD) to the organic nitrogen in particles above the nitracline and to zooplankton from the upper 50 m of the different phytoplankton communities sampled. Note that Sta. 23 was included in the MH1 group and Sta. 21 was included in the OC group (see text for details). The diazotroph contribution is calculated after Montoya et al. (2002) and Landrum et al. (2011) using the reference $\delta^{15}N$ values shown in the first row of this table. Italicized entries may reflect the impact of direct grazing on low $\delta^{15}N$ particles of a potentially non-diazotroph origin. See text for further details.

	Sta.	PN (%)	$Zoo_{200–500}$ (%)	$Zoo_{500–1000}$ (%)	$Zoo_{1000–2000}$ (%)	$Zoo_{2000–5000}$ (%)	$Zoo_{>5000}$ (%)
Reference $\delta^{15}N$ (‰)		−2/4.5	−2/3.7	−2/4.3	−2/5.1	−2/5.8	−2/4.7
Estuarine	4	*25 ± 26, n=2*	0 ± 2, *n*=3	0 ± 2, *n*=3	0 ± 0, *n*=3	*0 ± 0, n=3*	*14 ± 41, n=2*
	10	0 ± 12, *n*=2	—	—	—	—	—
	11	6, *n*=1	—	—	—	—	—
	14	21 ± 1, *n*=2	—	—	—	—	—
	16	21 ± 4, *n*=2	—	—	—	—	—
	17	0, *n*=1	—	—	—	—	—
Mesohaline 1	3	*43 ± 15, n=2*	0 ± 0, *n*=4	0 ± 0, *n*=4	0 ± 10, *n*=4	*0 ± 0, n=4*	*18 ± 56, n=4*
	9	22 ± 6, *n*=3	—	—	—	—	—
	23	*26 ± 10, n=3*	0 ± 0, *n*=7	0 ± 0, *n*=8	*8 ± 4, n=7*	*5 ± 17, n=8*	*15 ± 22, n=8*
Mesohaline 2	2	138*†±5, *n*=2	43 ± 8, *n*=3	44 ± 4, *n*=3	38 ± 10, *n*=3	35 ± 3, *n*=3	16 ± 4, *n*=3
	19	74 ± 2, *n*=2	47 ± 4, *n*=4	36 ± 8, *n*=4	36 ± 7, *n*=4	39 ± 3, *n*=4	25 ± 5, *n*=4
	25	86 ± 13, *n*=4	—	—	—	—	—
Oceanic	5	115*†±17, *n*=2	11 ± 8, *n*=4	1 ± 8, *n*=4	5 ± 5, *n*=4	*18 ± 3, n=4*	0 ± 2, *n*=4
	6	111*†±59, *n*=2	30 ± 9, *n*=4	23 ± 13, *n*=4	18 ± 8, *n*=4	*22 ± 6, n=4*	*7* ± 13, *n*=4
	7	103*† ±9, *n*=2	—	—	—	—	—
	8	108*† ±37, *n*=2	—	—	—	—	—2
	20	84 ± 13, *n*=2	53 ± 2, *n*=2	39 ± 2, *n*=2	26 ± 5, *n*=2	35 ± 1, *n*=2	13 ± 0, *n*=2
	21	26 ± 12, *n*=2	1 ± 2, *n*=2	0 ± 0, *n*=2	1 ± 4, *n*=2	11 ± 3, *n*=2	4 ± 4, *n*=2
	27	*76 ± 20, n=5*	48 ± 4, *n*=4	30 ± 8, *n*=4	35 ± 4, *n*=4	23 ± 12, *n*=4	*21 ± 23, n=4*
ES		*13 ± 15*	0 ± 2	0 ± 2	0 ± 0	0 ± 0	*14 ± 41*
*MH*1 incl. Sta. 23		*28 ± 11*	0 ± 0	0 ± 0	3 ± 8	*0 ± 21*	*16 ± 37*
*MH*2		86 ± 12†	45 ± 7	39 ± 8	37 ± 8	37 ± 4	21 ± 6
OC incl. Sta. 21		*79 ± 24*†	*29* ± 20	18 ± 18	18 ± 14	21 ± 9	9 ± 18

*Values of >100% diazotroph N may be artifacts due to a temporal uncoupling between NH_4^+ incorporation into PN but not into zooplankton
†Assuming 100% diazotroph N for MH2 Sta. 2, and OC Stas. 5, 6, 7, and 8 for average PN calculations.

1996). Besides the river plume, the onshore advection of nutrient rich North Brazilian Current water (Demaster and Pope 1996), and anticyclonic (warm core) and cyclonic (cold core) North Brazilian Current rings (Fratantoni and Richardson 2006) may have a marked impact on the hydrology and biological activity of the shelf and in offshore waters between the equator and 10°N.

Previous studies of the nutrient systematics in the Amazon River and its plume have shown nitrogen to be the most limiting nutrient for algal growth in both shelf (Demaster and Pope 1996) and offshore waters (Cooley and Yager 2006; Cooley et al. 2007). The Amazon River carries high concentrations of silicate (14–150 μmol L^{-1}) and phosphate (0.6–0.8 μmol L^{-1}) but nitrate concentrations of 12–23 μmol L^{-1} are low compared to other large rivers like the Pearl (Cai et al. 2004) or Mississippi Rivers (Dagg et al. 2004), where nitrate concentrations are typically higher than 75 μmol L^{-1}. Within the plume, this nutrient composition leads to strong N limitation of algal growth at the outer Amazon shelf (4–5°N) where silicate and phosphate concentrations remain high (Demaster and Pope 1996). Algal blooms are nevertheless present on the outer Amazon shelf during all seasons (summarized by Demaster and Pope 1996). The depletion of dissolved inorganic nitrogen we observed in the river plume (Fig. 3A) and the shoaling of the nitracline into surface waters at the ES stations (Fig. 4A) are both consistent with an important role for advective inputs of nitrate-rich subplume waters in supporting primary production on the shelf. The elevated ammonium concentrations we found throughout the water column at MH1 and MH2 stations also suggest that regenerated nutrients make an

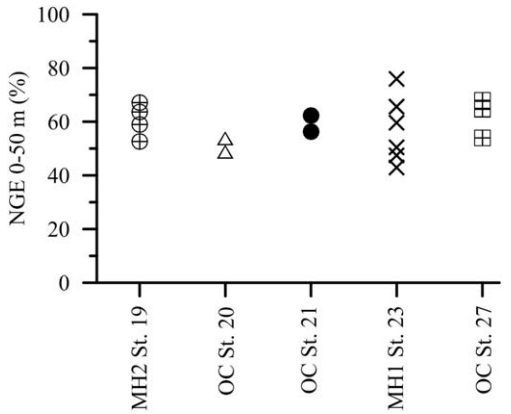

Fig. 10. Nitrogen based NGE (%) of the smallest zooplankton size fraction 200–500 μm in the upper 50 m of the water column. A single outlier of very high δ^{15}N zooplankton (8.4‰) has been excluded from the Sta. 23 data for this analysis.

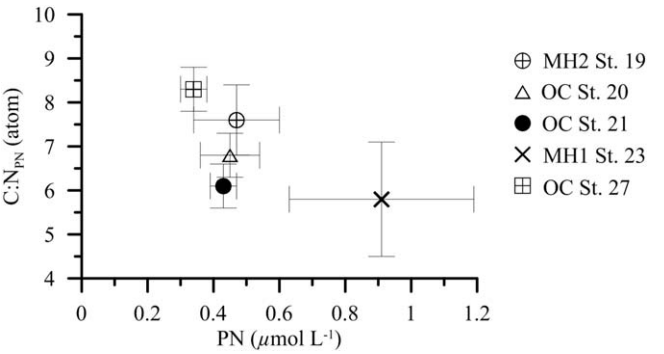

Fig. 11. Nitrogen concentration (μmol L^{-1}) vs. C: N (atom) ratios in particles above the nitracline as measure of food quantity and quality differences among stations with different nitrogen based net growth efficiencies according to Fig. 10.

important contribution to algal production, as suggested by Demaster and Pope (1996).

Beyond the shelf, the phosphate and silicate loads from the Amazon River plume support high biological production and carbon sequestration (Cooley and Yager 2006; Cooley et al. 2007). In offshore waters, N_2 fixation by diatom diazotroph associations (DDAs) can offset nitrogen limitation, promoting enhanced primary production and carbon drawdown (Subramaniam et al. 2008). The coincidence of high abundances of DDAs (Carpenter et al. 1999; Foster et al. 2007), high N_2 fixation rates (Subramaniam et al. 2008), enhanced DIC drawdown (Körtzinger 2003; Cooley et al. 2007), and low δ^{15}N values in sediment trap material collected at a depth of 200 m at a DDA plume station (Subramaniam et al. 2008) all provide evidence for the critical role of DDAs in the outer Amazon plume region beyond the shelf. Direct measurements of high N_2 fixation rates at the MH2 and OC stations, in combination with their deep nitraclines > 80 m depth (Fig. 4C,D) and the dominance of either DDAs (MH2) or *Synechococcus* spp. and *Trichodesmium* spp. (Goes et al. 2014) provide additional support for an important role of diazotroph nitrogen in the planktonic food web of the outer Amazon River plume and adjacent oceanic waters.

In the central tropical North Atlantic, inputs of DON, nitrate, or ammonium from atmospheric deposition may be similar in magnitude to inputs of N from N_2 fixation (Baker et al. 2007; Singh et al. 2013). We did not quantify atmospheric inputs of nitrogen but the high deposition rates of the manganese and iron (Chen and Siefert 2004; Tovar-Sanchez et al. 2006) in this region suggests that atmospheric deposition of nitrogenous nutrients deserves further investigation. Nonetheless, no wet deposition event occurred during cruise KN 197 and atmospheric dry deposition should have a broad regional impact that is unlikely to generate the finer-scale contrasts we found among the different phytoplankton communities in our study area.

Although loss of samples precluded direct measurement of the contribution of DON from the Amazon River to the nitrogen budget of the Plume, we used measurements of the concentration and δ^{13}C of DOC to constrain the potential contribution of riverine dissolved organic matter to the phytoplankton communities in our study area. The surface DOC concentration and δ^{13}C DOC values from Medeiros et al. (2015) show conservative behavior with respect to salinity (Figs. 7, 8), and a dissolved organic matter C: N ratio of 34 (Hedges et al. 1994) suggests that up to 4.6 μmol L^{-1} of nitrogen may have entered our study area as DON. Since DON varies in lability with reactive components like urea, dissolved free amino acids, and methylamines contributing only around 12% to the total DON pool (Bronk 2002), this provides an upper limit to the contribution of DON to the nutrient budget, with a small input of labile DON (0.55 μmol L^{-1}) relative to the inputs of nitrate via the river plume (12–23 μmol L^{-1}). DON is at most, a minor source of N supporting phytoplankton production in this system.

In summary, our nutrient and isotopic data as well as prior studies all imply that subthermocline nitrate and N_2 fixation are the primary sources of new nitrogen supporting production in our study region. We found no evidence that the Amazon is an important source of bioavailable nitrogen in the outer plume and adjacent oceanic waters.

Spatial and short term variation in the δ^{15}N of PN

We used variations in the δ^{15}N of PN with depth to delineate the contributions of different nitrogen sources to suspended particles and zooplankton in the water column. Temporal changes in δ^{15}N profiles from a single station helped us identify transient events that may affect our isotope budget calculations and obscure trophic relationships between PN and zooplankton.

N_2 fixation typically generates PN with a $\delta^{15}N$ of $-2‰$, but low $\delta^{15}N$ values can also arise through other processes. For example, phytoplankton uptake of subthermocline nitrate ($\delta^{15}N = 4.5‰$) may also produce low $\delta^{15}N$ PN values due to the isotopic fractionation associated with nitrate uptake ($\varepsilon = 5–10‰$; Montoya and McCarthy 1995; Waser et al. 1998). Nitrate uptake in the nitracline may, therefore, account for the minimum in $\delta^{15}N$ we commonly found associated with a maximum of PN or Chl. *a* near the base of the mixed layer (e.g., Stas. 3 and 23). Other stations (e.g., Stas. 9 and 25) showed a clear subsurface maximum in the $\delta^{15}N$ of PN. In a steady-state system, the upward injection of subthermocline nitrate supports phytoplankton uptake that progressively increases the $\delta^{15}N$ of the residual nitrate toward the top of the nitracline (Altabet 1996; Needoba et al. 2003), resulting in a strong gradient in $\delta^{15}N$ with depth. In effect, low subsurface values in the $\delta^{15}N$ of PN (e.g., at 40 m depth at Sta. 23) result from the early stages of consumption and fractionation of upwelling nitrate, producing strong ^{15}N depletion, while shallower $\delta^{15}N$ values approaching $8‰$ (Sta. 9) and $10‰$ (Sta. 25) reflect the integrated effect of consumption and ^{15}N enrichment of the residual upwelling nitrate (Montoya 2007).

Below the mixed layer, $\delta^{15}N$ PN tends to increase in concert with a decrease in PN concentration due to isotopic fractionation during remineralization (summarized in Montoya et al. 2002). This general pattern occurred at stations of all community types, including Estuarine Sta. 16, Mesohaline Stas. 3 and 23 (the anomalous DDA station), and Oceanic Sta. 21 (Fig. 8). The rates and mechanisms of particle export from the upper water column may differ among the three phytoplankton communities, with different impacts on the vertical distribution of $\delta^{15}N$ PN. Rapid sinking of particles should occur at sites dominated by diatoms due to ballasting by their high-density frustules, producing uniform $\delta^{15}N$ profiles (Fig. 8) such as we found at our Estuarine (Stas. 10, 11, 14, and 17) and Mesohaline stations (Sta. 19). In contrast, small cyanobacterial cells and cyanobacteria with gas vesicles will have a much slower sinking speed unless they form aggregates (Ploug 2008), allowing development of vertical structure in $\delta^{15}N$ that reflects local processes within the water column, as we observed at our other stations. These differences in sinking speed may also generate community specific patterns in ammonium distribution. We found the highest ammonium concentrations at MH1 and MH2 stations, where particles should have intermediate sinking speeds and vertical fluxes because the phytoplankton community was not dominated by large diatoms as at the ES stations, or very small cells or colonial cyanobacteria with gas vesicles as at the OC stations. Such intermediate sinking speeds provide opportunity for remineralisation of sinking particles leading to elevated ammonium concentrations in the water column.

Phytoplankton uptake of remineralized ammonium may also contribute to isotopic variation in the water column, though the fractionation factor for this process shows wide variation ($\varepsilon = 0–14‰$; Waser et al. 1999) depending on the nutrient status (N-stressed vs. N-replete) of the phytoplankton. Assimilation of regenerated ammonium can thus lead to $\delta^{15}N$ of PN values that are substantially lower than the $\delta^{15}N$ of the organic source materials (Montoya and McCarthy 1995; Waser et al. 1998), producing low $\delta^{15}N$ of PN values. Interestingly, we repeatedly measured $\delta^{15}N$ PN values as low as $-11‰$ (Fig. 8), and some of these low $\delta^{15}N$ values coincided with elevated ammonium concentrations in the water column (Stas. 2, 6, 19 and 25). Although atmospheric ammonium and nitrate are often depleted in ^{15}N (as low as $-12‰$, Baker et al. 2007) and could potentially contribute to our low water column $\delta^{15}N$ values, atmospheric dry deposition should have a broad regional impact and is unlikely to affect only MH1 and MH2 stations. Instead, the spatial distribution of our low $\delta^{15}N$ values and the presence of elevated ammonium concentrations below the river plume, are both consistent with local production of ammonium through remineralization and excretion driven by enhanced biological production in the plume. Elevated ammonium concentrations below the plume in offshore waters (Fig. 6B,C) also suggest that shoreward advection may play a key role in supplying ammonium to mesohaline communities on the shelf.

Repeated sampling at several stations revealed dynamic changes in the $\delta^{15}N$ of PN profiles on a time scale of hours to days (Fig. 8). In a heterogeneous system like the Amazon River plume, advection and tidal forcing can change the surface water masses present at a station within hours. In addition, cold- and warm-core eddies of the North Brazilian Current are common in this area (Fratantoni and Richardson 2006), and may contribute to the clear differences we found in the vertical structure of the $\delta^{15}N$ of PN among profiles taken at a single station, as well as driving shifts in nitracline depth as we found at Sta. 25. A temperature-salinity analysis using the approach of Bourlès et al. (1999a,b) and Kirchner et al. (2009) showed that such water mass changes can account for the dynamic changes in the $\delta^{15}N$ of PN we observed at multiple stations (Stas, 2, 6, 19, 20, 23, 25, and 27; Supporting Information Fig. S1).

In summary, the isotopic fractionation associated with assimilation of N_2, subthermocline nitrate, and regenerated ammonium, the characteristic sinking velocities of different phytoplankton groups, and changes in water mass all make important contributions to the vertical structure of the $\delta^{15}N$ of PN in the upper 100 m of the water column. Interestingly, the high $\delta^{15}N$ values typically associated with isotopic fractionation within the nitracline sometimes occurred well above the actual depth of the nitracline, (e.g., Stas. 21 and 23) suggesting that the $\delta^{15}N$ of PN can preserve a nitracline imprint generated during transit over the shelf, where nitracline depths are typically much shallower than in offshore

waters. Upward mixing of subthermocline nitrate was very important at our ES and MH1 type stations, as well as at OC Stas. 21 and 23. In contrast, MH2 and other OC stations were strongly impacted by the supply of diazotroph N and the remineralisation of regenerated ammonium.

Spatial and short term variation in zooplankton $\delta^{15}N$

The isotopic composition of PN will propagate into the zooplankton community through trophic interactions. Because zooplankton nitrogen is inherently less dynamic than phytoplankton/microbial nitrogen, zooplankton act as a low-pass filter and have an isotopic composition that integrates over the various sources of organic nitrogen supporting the heterotrophic components of the food web. Rapid (hours to days) changes in the $\delta^{15}N$ of particles at the base of the food web will propagate first into small, short-lived herbivores, then larger herbivores, while animals feeding at higher trophic positions as well as animals with a relatively long turnover time for body nitrogen should show little or no response to transient changes in the $\delta^{15}N$ of phytoplankton (Montoya 2007). These different time scales of N turnover and the ability of zooplankton to migrate vertically and to graze over a range of depths contribute to the relative invariance of the $\delta^{15}N$ of zooplankton compared to the $\delta^{15}N$ of PN at our stations (Fig. 9 and Supporting Information Fig. S3).

In contrast to previous observations from the Tropical North Atlantic, the Gulf of Mexico, and the Pacific (summarized by Montoya 2007), the $\delta^{15}N$ of zooplankton (like the $\delta^{15}N$ of PN) did not consistently show an inverse correlation with diazotroph abundance or high N_2 fixation rates. While the $\delta^{15}N$ of zooplankton was low at most *Trichodesmium* spp.-dominated oceanic stations (with the exception of Sta. 21), this was not true at all of the DDA-dominated MH stations where we sampled zooplankton (Fig. 9C1,C2). Despite high N_2 fixation rates at Stas. 2, 19, and 23 (Table 3), only Stas. 2 and 19 show low δ ^{15}N values in all zooplankton size fractions (Fig. 9). As noted above, nutrient concentrations differed between MH1 and MH2 stations, with high surface concentrations of Si and PO_4^{3-} at MH1 Stas. 3 and 23, while MH2 Stas. 2 and 19 had much lower concentrations of silicate and very low concentrations of phosphate at the surface. This pattern suggests that waters at Stas. 3 and 23 were advected offshore more recently, carrying diatoms and perhaps zooplankton with a relatively high $\delta^{15}N$ arising from production on the shelf supported by lateral (shoreward) inputs of subthermocline nitrate (see above). With time, we anticipate that waters from these two stations would come to resemble Stas. 2 and 19, where diazotrophy made a clear contribution to biomass, producing low $\delta^{15}N$ values throughout the planktonic food web.

Although zooplankton $\delta^{15}N$ is clearly linked to the $\delta^{15}N$ of suspended particles, three of our stations (Stas. 2, 5, and 6) showed low $\delta^{15}N$ values in PN but not zooplankton in the upper 100 m of the water column. This pattern suggests that the low $\delta^{15}N$ PN values at these stations resulted from transient events that had occurred so recently that the isotopic signature had not yet propagated into mesozooplankton. Similar offsets between the $\delta^{15}N$ of PN and zooplankton have been found in other dynamic systems like the Chesapeake Bay after a storm event (Montoya et al. 1991) and at an equatorial site in the tropical North Atlantic after an apparent upwelling event (Montoya et al. 2002).

In summary, the longer N turnover times and depth-integrated feeding behavior of zooplankton both contribute to the relatively invariant $\delta^{15}N$ of these animals compared to water column PN. Outliers in the zooplankton $\delta^{15}N$ profiles may reflect differential propagation of ^{15}N-perturbations at the base of the planktonic food web into different portions of the mesozooplankton community, though changes in zooplankton community composition may also contribute to the isotopic variation we observed.

Diazotroph N in particles and zooplankton

We used the distribution of stable nitrogen isotopes to assess the contribution of diazotroph N to suspended particles and zooplankton. A simple mass balance approach (e.g., Montoya et al. 2002) can unambiguously resolve only two isotopically distinct sources of N, but there are at least five sources of N that can potentially support production in the Amazon Plume: N_2 fixation (diazotrophy), upwelling of subthermocline nitrate, local remineralization of ammonium, inputs from the river, and atmospheric deposition. As noted above, atmospheric wet deposition did not take place during our cruise and atmospheric dry deposition should be relatively uniform over our study area, and would not account for the contrasts we found among stations. Our nutrient measurements, the distribution of DOC, as well as the analysis of Goes et al. (2014) all suggest that the river is a negligible source of N for biological production at outer plume stations north of 4°N (Fig. 3A). Diazotrophs are unevenly distributed in the Amazon plume system, and physical conditions (e.g., the depth of the nitracline) place a strong constraint on upwelling of subthermocline nitrate. As a result, N_2 fixation and upwelling of nitrate tend to dominate in different portions of our study area, while the potential for uptake of remineralized ammonium is greatest in areas with high surface productivity and in portions of the water column receiving substantial inputs of sinking organic matter. Because these sources are associated with distinct isotopic signatures and/or generate characteristic vertical patterns, we can use the $\delta^{15}N$ of different planktonic pools of N and a simple mass balance approach (Montoya et al. 2002) to estimate the contribution of different N sources to biological production above the nitracline. In doing so, we first assessed the relative contributions of N_2 fixation and upwelling of nitrate to the N budget, then evaluated the potential

for local inputs of remineralized ammonium to generate unusually low $\delta^{15}N$ values.

Our stations reflect a broad range of diazotrophic inputs to the N budget. For example, suspended particles at our MH2 and OC stations have generally low $\delta^{15}N$ values, which are consistent with the higher N_2 fixation rates we measured at these stations (Figs. 3-5). Particles at our ES stations have generally high $\delta^{15}N$ values, in keeping with the lowest rates of N_2 fixation we measured on this cruise. With the exception of Sta. 23, our MH1 stations fall between these two extremes, both in $\delta^{15}N$ and in rates of N_2 fixation. This overall pattern has been documented previously among oligotrophic (up to 100% diazotroph N in suspended particles) and more eutrophic (0–10% diazotroph N in suspended particles) areas in the Tropical North Atlantic (Montoya et al. 2002; Wannicke et al. 2010; Landrum et al. 2011) and the South China Sea (Loick et al. 2007).

In contrast to the relatively consistent isotopic systematics of our OC and ES stations, particles at stations with high abundances of DDAs and *Synechococcus* spp. showed wide variation in $\delta^{15}N$, including high $\delta^{15}N$ values above the nitracline (MH1 stations, Table 2). This pattern implies a significant input of sub-thermocline nitrate at stations where the *Hemiaulus/Richelia* association was present but not dominant (Goes et al. 2014) and where moderate to high N_2 fixation rates occurred (MH 1 stations, Table 3). The sub-thermocline nitrate contribution was much lower at stations dominated by DDAs (MH2 stations, Table 4), which is consistent with previous observations of a very strong reliance on N_2 fixation during a DDA bloom (Carpenter et al. 1999)

The low diazotroph contribution to PN above the nitracline at MH1 stations reflected the high abundance of asymbiotic diatoms at these stations (Goes et al. 2014). The only MH1 station with high rates of N_2 fixation was Sta. 23 (134 μmol N m^{-2} d^{-1} in the >10 μm size fraction), which had a deep nitracline (100 m, Fig. 4), making significant inputs of sub-thermocline nitrate into surface waters unlikely. The sea surface salinity, silicate, and phosphate distributions at the MH1 stations were all similar to those of the ES stations (Table 2), which suggests an advective input of surface shelf water containing particles with a high $\delta^{15}N$ signature derived from nitrate uptake on the shelf. The enhanced *Hemiaulus/Richelia* abundance (1927 cells L^{-1}, Yeung et al. 2012) and high N_2 fixation rates in the >10 μm size fraction at Sta. 23 indicate that DDAs were able to grow and fix N_2 in the presence of nitrate, which is similar to the growth of DDAs in the Mekong plume (Grosse et al. 2010). We also found appreciable N_2 fixation rates in the > 10 μm size fraction at ES stations (Table 3) with elevated *Hemiaulus/Richelia* abundance (up to 744 cells L^{-1}; R. A. Foster pers. comm.) and ambient DIN concentrations as high as 1–1.2 μmol L^{-1} (Stas. 4 and 16). These rates are similar to those found in the South China Sea off Vietnam (Voss et al. 2006). In this context, the frequency and intensity of nitrate injection into the mixed layer as well as the offshore advection from the shelf of seed populations of *Hemiaulus/Richelia* may all be critical aspects of the DDA niche in the Amazon Plume.

The movement of diazotroph N into the zooplankton community of the Amazon plume varied widely and reflected the diazotroph N contribution to PN. Generally small diazotroph contributions occurred at ES and MH1 stations (0–6%, excluding an outlier in zooplankton > 5000 μm from Sta. 4), intermediate contributions occurred at OC stations (9–23%), and the highest diazotroph contribution was found at MH2 stations (21–45%, Table 4). This general pattern has been documented previously among oligotrophic (up to 65% diazotroph N in epipelagic zooplankton) and more eutrophic (0–10% diazotroph N in epipelagic zooplankton) areas in the Western and Eastern Tropical North Atlantic (Montoya et al. 2002; Wannicke et al. 2010; Landrum et al. 2011; Hauss et al. 2013).

Diazotroph nitrogen contributions were not evenly distributed among zooplankton size fractions. At all MH2 and most oceanic stations, diazotroph N contribution was highest in the smallest size fractions and generally decreased with zooplankton size (Table 4). In contrast, a number of stations (ES Sta. 4, MH1 Stas. 3 and 23, and OC Stas. 5 and 21) showed a different pattern in which the diazotroph contribution to total nitrogen was highest in the larger size fractions (> 1000 μm, Table 4). These two patterns corroborate earlier suggestions that diazotroph N may enter the food web either via the microbial loop (all MH2 and most oceanic stations) or via direct grazing (at ES Sta. 4, MH1 Stas. 3 and 23, and OC Stas. 5, 21, 27) by small as well as by larger zooplankton (Montoya et al. 2002; Mulholland 2007; Raes et al. 2014).

NGE of zooplankton in the different communities

We used a novel isotopic approach to constrain NGE in three different plankton communities. In contrast to the classical K_2 approach, which is based on the difference in nitrogen: phosphorus ratios of the animal, its prey, and its excretion products (Le Borgne 1982 and references therein), our isotopic approach does not require incubation experiments.

The range of NGE values that we estimated for small mesozooplankton (43% to 76%, average 59 ± 10%, $n = 19$) falls in the upper portion of the range of values derived from the K_2 approach (18 to 71%) in the Eastern Tropical Atlantic and elsewhere (Le Borgne 1982 and references therein). Although we expected that direct grazing on diatoms and DDAs could result in more efficient nitrogen utilization, as suggested by Montoya et al. (2002) and Mulholland (2007), we found uniformly high NGEs for small mesozooplankton at all sites. Interestingly, this small range for NGEs compared to the results by Le Borgne (1982) occurred despite clear spatial differences in both food quantity (PN concentrations) and quality (C: N atomic ratios; Fig. 11).

Some modeling studies have generated NGEs up to 100% for animals under severe nitrogen stress (Anderson and

Hessen 1995). In contrast, models based on laboratory measurements of gross nitrogen growth efficiency of the calanoid copepods *Acartia tonsa* (Kiorboe 1989) and *Paracalanus parvus* (Checkley 1980) require a narrow range of nitrogen specific growth efficiencies (43.5% to 45.1%) and a variable net carbon growth efficiency to maintain stoichiometric homeostasis (Touratier et al. 1999; Touratier et al. 2001). Our comparatively narrow range of NGEs are more consistent with these model results but are on average 15% higher than those of Kiorboe (1989) and Checkley (1980). Both secondary production and export flux are highly sensitive to the value of NGE in marine ecosystem models (Anderson et al. 2013) but additional NGE measurements from different latitudes are needed to resolve whether NGEs of tropical zooplankton are generally higher than NGEs of mid and high latitude zooplankton.

We found no significant differences among communities in the scaling of zooplankton δ^{15}N with increasing animal size. This is surprising given that zooplankton community structure changed between the major regions of our study area (Steinberg unpubl. data) and implies that both trophic structure and the overall transfer efficiency of N through the food web were similar at all these stations. This finding also contrasts with an earlier suggestion that DDA-based food webs should show higher transfer efficiencies for N within the food web (Carpenter et al. 1999; Montoya et al. 2002).

Conclusions

Diazotroph N made a clear contribution to plankton biomass in our study region, which encompassed three different habitat types in the region of the Amazon Plume. Our data suggest that DDAs were able to flourish despite measurable ambient nitrate concentrations in surface waters and that the advection of seed populations from the shelf may play an important role in the formation of offshore DDA blooms in older plume waters. This pattern is consistent with model predictions of community succession along the Amazon River plume, which show the highest realized growth rates for DDAs in coastal regions, slightly lower rates in mesohaline regions, and much lower rates in the oligotrophic Atlantic (Stukel et al. 2014). Isotopic evidence for direct grazing on diazotrophs at ES and MH1 stations but not at MH2 stations is consistent with the model's outcome that grazing was an important control on coastal DDA populations, but that dilution of the grazer population in the mesohaline region released the DDAs from top down control and allowed blooms to develop in regions where mesohaline plume conditions persisted for at least several weeks (Stukel et al. 2014).

We used a stable isotope approach to estimate in situ NGEs of zooplankton communities without experimental manipulations. The determination of the food source and feeding history of zooplankton in the field remains challenging and our approach of excluding stations with variable δ^{15}N values in PN or zooplankton limited the number of food-consumer pairs available for estimating NGE. Nevertheless our results clearly confirm earlier laboratory experiments suggesting that the NGE of mesozooplankton is relatively invariant and independent of changes in nitrogen sources, food quality, and food abundance.

References

Agawin, N. S., M. Benavides, A. Busquets, P. Ferriol, L. J. Stal, and J. Arístegui. 2014. Dominance of unicellular cyanobacteria in the diazotrophic community in the Atlantic Ocean. Limnol. Oceanogr. **59**: 623–637.

Altabet, M. A. 1989. A time-series study of the vertical structure of nitrogen and particle dynamics in the Sargasso Sea. Limnol. Oceanogr. **34**: 1185–1201. doi:10.4319/lo.1989.34.7.1185

Altabet, M. A. 1996. Nitrogen and carbon isotopic tracers of the source and transformation of particles in the deep sea, p. 155–184. *In* V. Ittekkot, P. Schäfer, S. Honjo, and P. J. Depetris [eds.], Particle flux in the ocean. Wiley.

Altabet, M. A., and J. J. McCarthy. 1985. Temporal and spatial variation in the natural abundance of ^{15}N in PON from a warm–core ring. Deep-Sea Res. **32**: 755–772. doi:10.1016/0198-0149(85)90113-X

Anderson, T. R., and D. O. Hessen. 1995. Carbon or nitrogen limitation in marine copepods? J. Plankton Res. **17**: 317–331. doi:10.1093/plankt/17.2.317

Anderson, T. R., D. O. Hessen, A. Mitra, D. J. Mayor, and A. Yool. 2013. Sensitivity of secondary production and export flux to choice of trophic transfer formulation in marine ecosystem models. J. Mar. Sys. **125**: 41–53. doi:10.1016/j.jmarsys.2012.09.008

Bada, J. L., M. J. Schoeninger, and A. Schimmelmann. 1989. Isotopic fractionation during peptide bond hydrolysis. Geochim. Cosmochim. Acta **53**: 3337–3341. doi:10.1016/0016-7037(89)90114-2

Baker, A., K. Weston, S. Kelly, M. Voss, P. Streu, and J. Cape. 2007. Dry and wet deposition of nutrients from the tropical Atlantic atmosphere: Links to primary productivity and nitrogen fixation. Deep-Sea Res. **54**: 1704–1720. doi:10.1016/j.dsr.2007.07.001

Benner, R., B. Biddanda, B. Black, and M. McCarthy. 1997. Abundance, size distribution, and stable carbon and nitrogen isotopic compositions of marine organic matter isolated by tangential-flow ultrafiltration. Mar. Chem. **57**: 243–263. doi:10.1016/S0304-4203(97)00013-3

Berggreen, U., B. Hansen, and T. Kiørboe. 1988. Food size spectra, ingestion and growth of the copepod *Acartia tonsa* during development: Implications for determination of copepod production. Mar. Biol. **99**: 341–352. doi:10.1007/BF02112126

Bourlès, B., Y. Gouriou, and R. Chuchla. 1999a. On the circulation in the upper layer of the western equatorial

Atlantic. J. Geophysical Res. **104**: 21151–21170. doi:10.1029/1999JC900058

Bourlès, B., R. Molinari, E. Johns, W. Wilson, and K. Leaman. 1999b. Upper layer currents in the western tropical North Atlantic. J. Geophys. Res. **104**: 1361–1375. doi:10.1029/1998JC900025

Bronk, D. A. 2002. Dynamics of DON, p. 153–247. *In* D. A. Hansell and C. A. Carlson [eds.], Biogeochemistry of marine dissolved organic matter. Academic Press.

Cai, D. L., F. C. Tan, and J. M. Edmond. 1988. Sources and transport of particulate organic carbon in the Amazon River and estuary. Estuar. Coast. Shelf Sci. **26**: 1–14. doi:10.1016/0272-7714(88)90008-X

Cai, W.-J., and others 2004. The biogeochemistry of inorganic carbon and nutrients in the Pearl River estuary and the adjacent Northern South China Sea. C. Shelf Res. **24**: 1301–1319. doi:10.1016/j.csr.2004.04.005

Carpenter, E. J., H. R. Harvey, B. Fry, and D. G. Capone. 1997. Biogeochemical tracers of the marine cyanobacterium *Trichodesmium*. Deep-Sea Res. **44**: 27–38. doi:10.1016/S0967-0637(96)00091-X

Carpenter, E. J., J. P. Montoya, J. Burns, M. Mulholland, A. Subramanian, and D. G. Capone. 1999. Extensive bloom of a N_2-fixing symbiotic association (*Hemiaulis hauckii* and *Richelia intracellularis*) in the tropical Atlantic Ocean. Mar. Ecol. Prog. Ser. **185**: 273–283. doi:10.3354/meps185273

Carpenter, E. J., and D. G. Capone. 2008. Nitrogen fixation in the marine environment, p. 141–184. *In* D. G. Capone, D. A. Bronk, M. R. Mulholland, and E. J. Carpenter [eds.], Nitrogen in the marine environment. Elsevier.

Checkley, D. M. 1980. The egg production of a marine planktonic copepod in relation to its food supply: Laboratory studies1. Limnol. Oceanogr. **25**: 430–446. doi:10.4319/lo.1980.25.3.0430

Checkley, D. M., Jr., and C. A. Miller. 1989. Nitrogen isotope fractionation by oceanic zooplankton. Deep-Sea Res. **36**: 1449–1456. doi:10.1016/0198-0149(89)90050-2

Chen, Y., and R. L. Siefert. 2004. Seasonal and spatial distributions and dry deposition fluxes of atmospheric total and labile iron over the tropical and subtropical North Atlantic Ocean. J. Geophysical Res. **109**: D09305. doi:10.1029/2003JD003958

Coles, V. J., M. T. Brooks, J. Hopkins, M. R. Stukel, P. L. Yager, and R. R. Hood. 2013. The pathways and properties of the Amazon River Plume in the tropical North Atlantic Ocean. J. Geophysical Res. **118**: 6894–6913. doi:10.1002/2013JC008981

Cooley, S., and P. Yager. 2006. Physical and biological contributions to the western tropical North Atlantic Ocean carbon sink formed by the Amazon River plume. J. Geophys. Res. **111**: C08018. doi:10.1029/2005JC002954

Cooley, S. R., V. J. Coles, A. Subramaniam, and P. L. Yager. 2007. Seasonal variations in the Amazon plume-related atmospheric carbon sink. Global Biogeochemical Cycles **21**: GB3014. doi:10.1029/2006GB002831

Dabundo, R., and others 2014. The contamination of commercial $^{15}N_2$ gas stocks with ^{15}N–labeled nitrate and ammonium and consequences for nitrogen fixation measurements. PLoS One **9**: e110335. doi:10.1371/journal.pone.0110335

Dagg, M., R. Benner, S. Lohrenz, and D. Lawrence. 2004. Transformation of dissolved and particulate materials on continental shelves influenced by large rivers: Plume processes. Continental Shelf Res. **24**: 833–858. doi:10.1016/j.csr.2004.02.003

Demaster, D., and R. H. Pope. 1996. Nutrient dynamics in Amazon shelf waters: Results from AMASSEDS. Continental Shelf Res. **16**: 263–289. doi:10.1016/0278-4343(95)00008-O

Ellis, E. E., and others 2012. Factors controlling water-column respiration in rivers of the central and southwestern Amazon Basin. Limnol. Oceanogr. **57**: 527–540. doi:10.4319/lo.2012.57.2.0527

Foster, R. A., A. Subramaniam, C. Mahaffey, E. J. Carpenter, D. G. Capone, and J. P. Zehr. 2007. Influence of the Amazon River Plume on distributions of free-living and symbiotic cyanobacteria in the western tropical north Atlantic Ocean. Limnol. Oceanogr. **52**: 517–532. doi:10.4319/lo.2007.52.2.0517

Fratantoni, D. M., and P. L. Richardson. 2006. The evolution and demise of north Brazil current rings. J. Phys. Oceanogr. **36**: 1241–1264. doi:10.1175/JPO2907.1

Frazer, T. K., R. M. Ross, L. B. Quetin, and J. P. Montoya. 1997. Turnover of carbon and nitrogen during growth of larval krill, *Euphausia superba*: A stable isotope approach. J. Exp. Mar. Biol. Ecol. **212**: 259–275. doi:10.1016/S0022-0981(96)02740-2

Fry, B., and E. B. Sherr. 1984. $\delta^{13}C$ measurements as indicators of carbon flow in marine and freshwater ecosystems. Contrib. Mar. Sci. **27**: 13–47. doi:10.1007/978-1-4612-3498-2_12

Fry, B., and R. B. Quiñones. 1994. Biomass spectra and stable isotope indicators of trophic level in zooplankton of the northwest Atlantic. Mar. Ecol. Prog. Ser. **112**: 201–204.

Gannes, L. Z., D. M. O'Brien, and C. Martinez Del Rio. 1997. Stable isotopes in animal ecology: Assumptions, caveats, and a call for more laboratory experiments. Ecology **78**: 1271–1276. doi:10.2307/2265878

Goering, J., V. Alexander, and N. Haubenstock. 1990. Seasonal variability of stable carbon and nitrogen isotope ratios of organisms in a North Pacific Bay. Estuar. Coast. Shelf Sci. **30**: 239–260. doi:10.1016/0272-7714(90)90050-2

Goes, J. I., and others 2014. Influence of the Amazon River discharge on the biogeography of phytoplankton communities in the Western Tropical North Atlantic. Prog. Oceanogr. **120**: 29–40. doi:10.1016/j.pocean.2013.07.010

Grosse, J., D. Bombar, H. Nhu Doan, L. Ngoc Nguyen, and M. Voss. 2010. The Mekong River plume fuels nitrogen fixation and determines phytoplankton species distribution in the South China Sea during low-and high-discharge season. Limnol. Oceanogr. **55**: 1668. doi:10.4319/lo.2010.55.4.1668

Hauss, H., J. M. Franz, T. Hansen, U. Struck, and U. Sommer. 2013. Relative inputs of upwelled and atmospheric nitrogen to the eastern tropical North Atlantic food web: Spatial distribution of δ^{15} N in mesozooplankton and relation to dissolved nutrient dynamics. Deep-Sea Res. **75**: 135–145. doi:10.1016/j.dsr.2013.01.010

Hedges, J. I., and others 1994. Origins and processing of organic matter in the Amazon River as indicated by carbohydrates and amino acids. Limnol. Oceanogr. **39**: 743–761. doi:10.4319/lo.1994.39.4.0743

Hutchins, D. A., and others 2007. CO_2 control of *Trichodesmium* N_2 fixation, photosynthesis, growth rates, and elemental ratios: Implications for past, present, and future ocean biogeochemistry. Limnol. Oceanogr. **52**: 1293–1304. doi:10.4319/lo.2007.52.4.1293

Kiorboe, T. 1989. Phytoplankton growth rate and nitrogen content: Implications for feeding and fecundity in a herbivorous copepod. Mar. Ecol. Prog. Ser. **55**: 229–234. doi:10.3354/meps055229

Kirchner, K., M. Rhein, S. Hüttl-Kabus, and C. W. Böning. 2009. On the spreading of South Atlantic Water into the northern hemisphere. J. Geophys. Res. **114**: C05019. doi:10.1029/2008JC005165

Knapp, A. N., P. J. Di Fiore, C. Deutsch, D. M. Sigman, and F. Lipschultz. 2008. Nitrate isotopic composition between Bermuda and Puerto Rico: Implications for N_2 fixation in the Atlantic Ocean. Global Biogeochem. Cycles **22**: GB3014. doi:10.1029/2007GB003107

Körtzinger, A. 2003. A significant CO_2 sink in the tropical Atlantic Ocean associated with the Amazon River plume. Geophys. Res. Lett. **30**: 2287. doi:10.1029/2003GL018841

Landrum, J. P., M. A. Altabet, and J. P. Montoya. 2011. Basin-scale distributions of stable nitrogen isotopes in the subtropical North Atlantic Ocean: Contribution of diazotroph nitrogen to particulate organic matter and mesozooplankton. Deep-Sea. Res. I **58**: 615–625. doi:10.1016/j.dsr.2011.01.012

Le Borgne, R. 1982. Zooplankton production in the eastern tropical Atlantic Ocean: Net growth efficiency and P: B in terms of carbon, nitrogen, and phosphorus. Limnol. Oceanogr. **27**: 681–698. doi:10.4319/lo.1982.27.4.0681

Lentz, S. J. 1995. The Amazon River plume during AMASSEDS: Subtidal current variability and the importance of wind forcing. J. Geophys. Res. **100**: 2377–2390. doi:10.1029/94JC00343

Loick, N., J. W. Dippner, H. N. Doan, I. Liskow, and M. Voss. 2007. Pelagic nitrogen dynamics in the Vietnamese upwelling area according to stable nitrogen and carbon isotope data. Deep-Sea Res. I **54**: 596–607. doi:10.1016/j.dsr.2006.12.009

Loick-Wilde, N., J. Dutz, A. Miltner, M. Gehre, J. P. Montoya, and M. Voss. 2012. Incorporation of nitrogen from N_2 fixation into amino acids of zooplankton. Limnol. Oceanogr. **57**: 199–210. doi:10.4319/lo.2012.57.1.0199

Martínez Del Rio, C., N. Wolf, S. A. Carleton, and L. Z. Gannes. 2009. Isotopic ecology ten years after a call for more laboratory experiments. Biol. Rev. **84**: 91–111. doi:10.1111/j.1469-185X.2008.00064.x

McClelland, J. W., C. M. Holl, and J. P. Montoya. 2003. Nitrogen sources to zooplankton in the Tropical North Atlantic: Stable isotope ratios of amino acids identify strong coupling to N_2-fixation. Deep-Sea Res. I **50**: 849–861. doi:10.1016/S0967-0637(03)00073-6

Medeiros, P. M., and others 2015. Fate of the Amazon River dissolved organic matter in the tropical Atlantic Ocean. Global Biogeochem. **29**: 677–690. doi:10.1002/2015GB005115

Minagawa, M., and E. Wada. 1984. Stepwise enrichment of ^{15}N along food chains: Further evidence and the relation between δ^{15}N and animal age. Geochim. Cosmochim. Acta **48**: 1135–1140. doi:10.1016/0016-7037(84)90204-7

Minagawa, M., and E. Wada. 1986. Nitrogen isotope ratios of red tide organisms in the East China Sea: A characterization of biological nitrogen fixation. Mar. Chem. **19**: 245–249. doi:10.1016/0304-4203(86)90026-5

Mitra, A., and others 2014. Bridging the gap between marine biogeochemical and fisheries sciences; configuring the zooplankton link. Prog. Oceanogr. **129**: 176–199. doi:10.1016/j.pocean.2014.04.025

Mitsui, A., S. Kumazawa, A. Takahashi, H. Ikemoto, S. Cao, and T. Arai. 1986. Strategy by which nitrogen-fixing unicellular cyanobacteria grow photoautotrophically. Nature **323**: 720–722. doi:10.1038/323720a0

Mohr, W., T. Grosskopf, D. W. R. Wallace, and J. La Roche. 2010. Methodological underestimation of oceanic nitrogen fixation rates. Plos One **5**: e12583. doi:10.1371/journal.pone.0012583

Moisander, P. H., R. A. Beinart, M. Voss, and J. P. Zehr. 2008. Diversity and abundance of diazotrophs in the South China Sea during intermonsoon. ISME J. **2**: 954–967. doi:10.1038/ismej.2008.51

Montoya, J. P. 2007. Natural abundance of ^{15}N in marine planktonic ecosystems, p. 176–201. *In* R. Michener and K. Lajtha [eds.], Stable Isotopes in ecology and environmental science. Methods in ecology. Blackwell.

Montoya, J. P. 2008. Nitrogen stable isotopes in marine environments, p. 1277–1302. *In* D. G. Capone, E. J. Carpenter, M. R. Mulholland, and D. A. Bronk [eds.], Nitrogen in the marine environment. Academic Press.

Montoya, J. P., S. G. Horrigan, and J. J. McCarthy. 1991. Rapid, storm-induced changes in the natural abundance

of ^{15}N in a planktonic ecosystem. Geochim. Cosmochim. Acta **55**: 3627–3638. doi:10.1016/0016-7037(91)90060-I

Montoya, J. P., P. H. Wiebe, and J. J. McCarthy. 1992. Natural abundance of ^{15}N in particulate nitrogen and zooplankton in the Gulf Stream region and Warm-Core Ring 86A. Deep-Sea Res. **39**: S363–S392. doi:10.1016/S0198-0149(11)80020-8

Montoya, J. P., and J. J. McCarthy. 1995. Nitrogen isotope fractionation during nitrate uptake by marine phytoplankton in continuous culture. J. Plankton Res. **17**: 439–464. doi:10.1093/plankt/17.3.439

Montoya, J. P., M. Voss, P. Kaehler, and D. G. Capone. 1996. A simple, high precision, high sensitivity tracer assay for dinitrogen fixation. Appl. Environ. Microbiol. **62**: 986–993.

Montoya, J. P., E. J. Carpenter, and D. G. Capone. 2002. Nitrogen fixation and nitrogen isotope abundances in zooplankton of the oligotrophic North Atlantic. Limnol. Oceanogr. **47**: 1617–1628. doi:10.4319/lo.2002.47.6.1617

Mulholland, M. R. 2007. The fate of nitrogen fixed by diazotrophs in the ocean. Biogeosciences **4**: 37–51. doi:10.5194/bg-4-37-2007

Needoba, J. A., N. A. D. Waser, P. J. Harrison, and S. E. Calvert. 2003. Nitrogen isotope fractionation by 12 species of marine phytoplankton during growth on nitrate. Mar. Ecol. Prog. Ser. **255**: 81–91. doi:10.3354/meps255081

O'Neil, J. M., P.M. Metzler, and P.M. Glibert. 1995. Ingestion of $^{15}N_2$ labelled *Trichodesmium* sp. and ammonium regeneration by the harpacticoid copepod *Macrosetella gracilis*. Mar. Biol. **126**: 89–96. doi:10.1007/BF00350763

Paerl, H. W., and J. Huisman. 2008. Climate. Blooms like it hot. Science **320** 57–58. doi:10.1126/science.1155398

Peterson, B. J., and B. Fry. 1987. Stable isotopes in ecosystem studies. Annu. Rev. Ecol. Syst. **18**: 293–320. doi:10.1146/annurev.es.18.110187.001453

Ploug, H. 2008. Cyanobacterial surface blooms formed by *Aphanizomenon* sp. and *Nodularia spumigena* in the Baltic Sea: Small-scale fluxes, pH, and oxygen microenvironments. Limnol. Oceanogr. **53**: 914–921. doi:10.4319/lo.2008.53.3.0914

Raes, E. J., Waite, A. M., McInnes, A. S., Olsen, H., Nguyen, H. M., Hardman-Mountford, N., and P. A. Thompson. 2014. Changes in latitude and dominant diazotrophic community alter N_2 fixation. Mar. Ecol. Prog. Ser. **516**: 85–102. doi:10.3354/meps11009

Ramesh, R., and A. Singh. 2010. Isotopic fractionation in open systems: Application to organic matter decomposition in ocean and land. Curr. Sci. **98**: 406–411.

Schwamborn, R., W. Ekau, M. Voss, and U. Saint-Paul. 1999. Stable isotope composition of particulate organic matter and zooplankton in northeast Brazilian shelf waters. Arch. Fish. Mar. Res . **201**: 47210.

Singh, A., M. Lomas, and N. Bates. 2013. Revisiting N_2 fixation in the North Atlantic Ocean: Significance of deviations from the Redfield Ratio, atmospheric deposition and climate variability. Deep-Sea Res. II **93**: 148–158. doi:10.1016/j.dsr2.2013.04.008

Steinberg, D. K., and G. K. Saba. 2008. Nitrogen consumption and metabolism in marine zooplankton, p. 1135–1196. *In* D. G. Capone, D. A. Bronk, M. R. Mulholland, and E. J. Carpenter [eds.], Nitrogen in the marine environment. Elsevier Academic Press.

Steinberg, D. K., M. W. Lomas, and J. S. Cope. 2012. Long-term increase in mesozooplankton biomass in the Sargasso Sea: Linkage to climate and implications for food web dynamics and biogeochemical cycling. Global Biogeochem. Cycles **26**: GB1004. doi:10.1029/2010GB004026

Stukel, M. R., V. J. Coles, M. T. Brooks, and R. R. Hood. 2014. Top-down, bottom-up and physical controls on diatom-diazotroph assemblage growth in the Amazon River plume. Biogeosciences **11**: 3259–3278. doi:10.5194/bg-11-3259-2014

Subramaniam, A., and others 2008. Amazon River enhances diazotrophy and carbon sequestration in the tropical North Atlantic Ocean. PNAS **105**: 10460–10465. doi:10.1073/pnas.0710279105

Taylor, B. W., and others 2007. Improving the fluorometric ammonium method: Matrix effects, background fluorescence, and standard additions. J. North Am. Benthol. Soc. **26**: 167–177. doi:10.1899/0887-3593(2007)26[167:ITFAMM]2.0.CO;2

Touratier, F., L. Legendre, and A. Vézina. 1999. Model of copepod growth influenced by the food carbon: Nitrogen ratio and concentration, under the hypothesis of strict homeostasis. J. Plankton Res. **21**: 1111–1132. doi:10.1093/plankt/21.6.1111

Touratier, F., J. G. Field, and C. L. Moloney. 2001. A stoichiometric model relating growth substrate quality (C:N:P ratios) to N:P ratios in the products of heterotrophic release and excretion. Ecol. Model. **139**: 265–291. doi:10.1016/S0304-3800(01)00237-X

Tovar-Sanchez, A., and others 2006. Effects of dust deposition and river discharges on trace metal composition of *Trichodesmium* spp. in the tropical and subtropical North Atlantic Ocean. Limnol. Oceanogr. **51**: 1755–1761. doi:10.4319/lo.2006.51.4.1755

Turner, J. 1980. Buoyancy effects in fluids. Buoyancy effects in fluids, by JS turner, p. 382. ISBN 0521297265. Cambridge, UK: Cambridge Univ. Press.

Voss, M., D. Bombar, N. Loick, and J. W. Dippner. 2006. Riverine influence on nitrogen fixation in the upwelling region off Vietnam, South China Sea. Geophys. Res. Lett. **33**: L07604. doi:10.1029/2005GL025569

Wannicke, N., I. Liskow, and M. Voss. 2010. Impact of diazotrophy on N stable isotope signatures of nitrate and particulate organic nitrogen: Case studies in the northeastern tropical Atlantic Ocean. Isotopes Environ Health Stud **46**: 337–354. doi:10.1080/10256016.2010.505687

Waser, N. A. D., P. J. Harrison, B. Nielsen, S. E. Calvert, and D. H. Turpin. 1998. Nitrogen isotope fractionation during the uptake and assimilation of nitrate, nitrite, ammonium, and urea by a marine diatom. Limnol. Oceanogr. **43**: 215–224. doi:10.4319/lo.1998.43.2.0215

Waser, N. A., and others 1999. Nitrogen isotopic fractionation during a simulated diatom spring bloom: Importance of N-starvation in controlling fractionation. Mar. Ecol. Prog. Ser. **179**: 291–296. doi:10.3354/meps179291

Waser, N. A. D., W. G. Harrison, E. J. H. Head, B. Nielsen, V. A. Lutz, and S. E. Calvert. 2000. Geographic variations in the nitrogen isotope composition of surface particulate nitrogen and new production across the North Atlantic Ocean. Deep-Sea Res. I **47**: 1207–1226. doi:10.1016/S0967-0637(99)00102-8

Yeung, L. Y., and others 2012. Impact of diatom-diazotroph associations on carbon export in the Amazon River plume. Geophys. Res. Lett. **39**: L18609. doi:10.1029/2012GL053356

Acknowledgments

We thank the captain and crew of R/V *Knorr* and Patricia L. Yager for the organization of the cruise. We gratefully acknowledge the assistance of Joe Cope, Miram Gleiber, and Jason Landrum in MOCNESS sample processing. We also thank Julie Gonzalez for her help during the mass spectrometry measurements as well as Katie Geddes, Princy Kuriakose, and Ryan W. Wong for their help during lab-based processing of the zooplankton samples. Joaquim I. Goes, Patricia L. Yager, and especially Arvind Singh and an anonymous reviewer helped to significantly improve an earlier version of this manuscript with their constructive comments and suggestions. This work was supported by a German Research Foundation grant (Lo1820/1-1) to NLW and United States National Science Foundation grants OCE-934073 (DGC), OCE-0933975 (VJC), OCE-0934036 (DKS), OCE-0934025 (JPM), and OCE-0934095 (PLY). PMM gratefully acknowledges Gordon and Betty Moore Foundation (GBMF-MMI-2293 and 2928) for the financial support provided to this study.

Submitted 7 February 2015
Revised 21 July 2015, 9 October 2015
Accepted 13 October 2015

Associate editor: Anya Waite